INFORMATION TO USERS

This reproduction was made from a copy of a manuscript sent to us for publication and microfilming. While the most advanced technology has been used to photograph and reproduce this manuscript, the quality of the reproduction is heavily dependent upon the quality of the material submitted. Pages in any manuscript may have indistinct print. In all cases the best available copy has been filmed.

The following explanation of techniques is provided to help clarify notations which may appear on this reproduction.

1. Manuscripts may not always be complete. When it is not possible to obtain missing pages, a note appears to indicate this.

2. When copyrighted materials are removed from the manuscript, a note appears to indicate this.

3. Oversize materials (maps, drawings, and charts) are photographed by sectioning the original, beginning at the upper left hand corner and continuing from left to right in equal sections with small overlaps. Each oversize page is also filmed as one exposure and is available, for an additional charge, as a standard 35mm slide or in black and white paper format.*

4. Most photographs reproduce acceptably on positive microfilm or microfiche but lack clarity on xerographic copies made from the microfilm. For an additional charge, all photographs are available in black and white standard 35mm slide format.*

*For more information about black and white slides or enlarged paper reproductions, please contact the Dissertations Customer Services Department.

U·M·I Dissertation Information Service

University Microfilms International
A Bell & Howell Information Company
300 N. Zeeb Road, Ann Arbor, Michigan 48106

8629739

Sidhu, Jagjeet Singh

ELECTROMAGNETIC BACKSCATTERING FROM A LAYER OF DISC SCATTERERS USING DISCRETE APPROACH AND RADIATIVE TRANSFER THEORY

City University of New York PH.D. 1986

University
Microfilms
International 300 N. Zeeb Road. Ann Arbor. MI 48106

Copyright 1986

by

Sidhu, Jagjeet Singh

All Rights Reserved

PLEASE NOTE:

In all cases this material has been filmed in the best possible way from the available copy. Problems encountered with this document have been identified here with a check mark __✓__.

1. Glossy photographs or pages _____
2. Colored illustrations, paper or print _____
3. Photographs with dark background _____
4. Illustrations are poor copy _____
5. Pages with black marks, not original copy _____
6. Print shows through as there is text on both sides of page _____
7. Indistinct, broken or small print on several pages __✓__
8. Print exceeds margin requirements _____
9. Tightly bound copy with print lost in spine _____
10. Computer printout pages with indistinct print _____
11. Page(s) _____ lacking when material received, and not available from school or author.
12. Page(s) _____ seem to be missing in numbering only as text follows.
13. Two pages numbered _____. Text follows.
14. Curling and wrinkled pages _____
15. Dissertation contains pages with print at a slant, filmed as received _____
16. Other _____

_____

_____

University
Microfilms
International

ELECTROMAGNETIC BACKSCATTERING FROM A LAYER OF DISC SCATTERERS USING DISCRETE APPROACH AND RADIATIVE TRANSFER THEORY

by

JAGJEET SINGH SIDHU

A dissertation submitted to the Graduate Faculty in Engineering in partial fulfillment of the requirements for the degree of Doctor of Philosophy, The City University of New York.

1986

© 1986

JAGJEET SINGH SIDHU

All Rights Reserved

This manuscript has been read and accepted for the Graduate Faculty in Engineering in satisfaction of the dissertation requirement for the degree of Doctor of Philosophy.

9/22/86
Date

Chair of Examining Committee

9/23/86
Date

Executive Officer

Frederick E. Thau

Shee-Ming Chen

Willard J. Pierson

Supervisory Committee

The City University of New York

Abstract

ELECTROMAGNETIC BACKSCATTERING FROM A LAYER OF DISC SCATTERERS USING DISCRETE APPROACH AND RADIATIVE TRANSFER THEORY

by

Jagjeet Singh Sidhu

Advisor: Professor George Eichmann

Electromagnetic backscattering from a vegetation layer over a flat lossy ground is studied. The vegetated region is composed of leaves which are modelled by lossy dielectric discs. The vegetation components are assumed to have random placement and specified orientation statistics.

First, a case of single scattering from Rayleigh scatterers is studied. The problem is solved by finding the mean field in the vegetated region by using the Foldy approximation and a two-variable technique. Simple expressions are given for the skin depth of the mean wave. Following this, the distorted Born approximation is used to calculate the backscattering coefficients.

To study the effects of multiple scattering, the Radiative Transfer Theory with a Rayleigh scattering model is used. The radiative transfer equation and the boundary conditions are first formulated into the integral equations form. The Fourier series expansion in the azimuth direction is used to eliminate the Ø-dependence from the radiative transfer equations. Then the set of equations without the Ø-dependence are solved using the method of Gaussian quadrature.

Formulas for co-polarized and cross-polarized backscattering coefficients are derived and numerical results for the backscattering coefficients as a function of the incidence angle are presented for different layer depths and leaf configurations.

ACKNOWLEDGMENTS

I would like to express my sincere gratitude to Prof. George Eichmann for his continued guidance, support and patience during the preparation of this thesis. I would also like to express my deepest appreciation to Prof. Roger Lang of George Washington University, Washington, D.C. for his consultation time, help and encouragement during all phases of this work.

Special thanks to my best friend and wife Rani for her patience, support and understanding during all these years. Finally, thanks to Leena and Misty for being source of encouragement and simply just being around.

To My Parents

TABLE OF CONTENTS

LIST OF ILLUSTRATIONS

CHAPTER 1

INTRODUCTION

The problem of wave propagation and scattering in the atmosphere and biological media has become increasingly important in recent years, particularly in the remote-sensing and detection area. To describe wave propagation in random media one has to use statistical characteristics of the media and a combination of simplifying assumptions regarding propagation conditions. These assumptions relate to the mechanism of wave scattering and the properties of the statistical medium.

1.1 RANDOM MEDIA SINGLE SCATTERING TECHNIQUE

In the past, electromagnetic scattering from a collection of discrete scatterers has been modelled by continuous and discrete random medium techniques. In the continuous case, the random medium is modelled by assuming that its permittivity $\epsilon(\bar{x})$ is a random process whose moments are known. The average backscattering cross section is then calculated from the knowledge of the statistics of $\epsilon(\bar{x})$. Usually, only the mean and correlation of the permittivity are required. The analysis of this problem can then proceed in a number of different ways. One method involves calculating the mean field,

using it to define an equivalent medium and then employing single scattering in the equivalent medium. In active remote sensing applications from terrain, the technique has been applied by a number of authors[10,11,12,14,34,50].

A typical approach in the continuous media case is to determine the coherent(mean) wave in the form of Dyson's equation. Dyson's equation expresses the mean field in terms of an infinite series and so must be approximated. The most commonly used approximation is the so-called bilocal approximation where only the first term in the infinite series is considered. The bilocally approximated mean field has been calculated for different configurations by various authors [1,21,25]. Another commonly used approximation to the Dyson's equation is the non-linear approximation in which more multiple scattering terms are included.

The Beth-Salpeter equation is an exact equation for the second moment of the field. However, the intensity operator is in the form of an infinite series, and most of the time it is approximated by the ladder-approximation. The ladder approximation accounts for multiple scattering of the mean field intensities by retaining only the mean fields and the conjugate mean fields that propagate in the same direction and within a correlation length of each other.

In the discrete random media technique, the individual objects, such as leaves, are characterized by their scattering cross sections or dipole moments. Each object is then given a random placement and orientation. An approximate

equation for the mean field has been obtained in both the scalar and vector cases[9,15,30,44,47]. A scalar equation for the correlation that can be applied to electromagnetic particles having polarization preserving properties has been obtained by Twersky[45]. Twersky[46], has found approximate solutions to this equation when the distribution of particles is sparse. Ishimaru[16], has found solutions to the correlation equation by employing the diffusion approximation.

The distorted Born approximation technique to find the correlation of the field by viewing the scatterers as being embedded in an equivalent medium and then using single scattering theory has been employed by Taylor[40] and Rosenbaum and Bowles[34].

For vegetation modelling, Du and Peake[8], employed the Born approximation to obtain the average backscattering coefficients. The technique employed by them is limited to low frequencies and thin vegetation layers. Lang and Sokolakis[26], avoided some of the restrictions inherent in the Born approximation, by taking into account the decay of the incident and scattered waves in the vegetated medium. This was done by finding an equivalent dielectric constant for the vegetated medium and embedding the spherical scatterers in it. Lang[27], has extended this work for spherical scatterers having arbitrary shapes. The method was applied to half space of discs. The major advantage of this approach is that most of the model parameters are directly related to the ground condition measurements.

The single scattering part of the present work is extension of the half-space problem to a layer problem with vegetation thickness 'd'. The underlying ground effects for different types of ground are taken into considerations. The backscattering coefficient has been studied as a summation of separate components σ^o_{pqd} , σ^o_{pqdr} and σ^o_{pqr} , where σ^o_{pqd} is the direct backscattering from the scatterer, σ^o_{pqdr} is the scattering and single reflection from the ground, and σ^o_{pqr} is the scattering and double reflection from the ground. These separate terms have been plotted along with the total back-scattering coefficient to show the relative effects of the underlying ground.

1.2 MULTIPLE SCATTERING - RADIATIVE TRANSPORT APPROACH

Another technique used to obtain the scattered fields from a continuous random medium is the radiative transport approach. Here, the transport equations are obtained in terms of the statistics of $\epsilon(\bar{x})$ as by Tsang and Kong[41]. Scatter-ing from a vegetation like half space has been studied using strong fluctuation random medium theory by Tsang and Kong[42] The radiative transfer theory is also applied within the Rayleigh approximation to calculate the backscattering cross section of a layer of randomly positioned and oriented small ellipsoids by Tsang et. al[43].

In the case when the medium correlation length is large

in comparison to wave length, de Wolf[7] and Ito and Adachi [17], have developed a multiple-forward and single-backscatter technique. Using all four Stokes parameters, Shin and Kong[37] calculated the backscattering cross sections by means of iterative and numerical approaches for spherical Rayleigh scatterers.

The second part of this work is an extension of this approach for disc scatterers. The iterative approach gives closed form solutions that are valid when the effect of scattering is small (small albedo). The radiative transfer equations and the boundary conditions are first cast into integral equations form. Then an iterative process is applied to solve the integral equations. A Fourier-series expansion in the azimuthal direction is used to eliminate the azimuthal Ø dependence from the radiative transfer equations. Then, the set of equations without the Ø dependence is solved using the method of Gaussian quadrature.

The numerical solutions are compared by plotting backscattering cross sections under different configurations. The results are matched with experimental data collected from vegetation fields by Fung and Ulaby[11] and Fung[12] for different types of vegetation. The comparison between the theory and data shows general agreements for both level and angular trends, indicating promise in the use of these backscatter models for explaining vegetation scattering and ground effects.

CHAPTER 2

2.0 SINGLE SCATTERING - A DISCRETE APPROACH

In this chapter, electromagnetic scattering from a collection of discrete scatterers in a layered media is modelled by a discrete random media technique. In this technique, the individual objects, such as leaves, stems etc. are characterized by their scattering cross sections or dipole moments. Each object is then given a random placement and orientation.

Although exact solutions have been obtained for the mean field and Green's function by Schesser and Eichmann[35], the complexities of these equations makes it quite impractical to compute the backscattering coefficients without resorting to some simplifying assumptions. In this work, a two-variable method has been used to obtain the mean field and Green's function. In this method, a small ordering factor 'δ' is introduced for the equivalent medium permittivity $\bar{\bar{\epsilon}}_r=\bar{\bar{I}}+\delta\bar{\bar{a}}$, where $\underline{a}$ is the average polarizability tensor. Since 'δ' is dependent upon particle density, a sparse distribution, $|\delta\bar{\bar{a}}|<<1$, is assumed.

An equation for the mean field is obtained by employing the Foldy technique and using a two-variable perturbation method. In the case of sparsely distributed scatterers the mean field equations for a horzontally polarized incident wave are derived. Then results for horizontally and vertically polarized incoming waves are combined into general

expressions for the mean wave in different regions of the layered media.

An equivalent dielectric constant for the scattering region is determined by means of this mean field. Then Distorted Born approximation theory for single scattering is employed to find the correlation of the field by assuming that the scatterers are embedded in the equivalent medium.

The dyadic green's function derived in Appendix A is used to find the relation between the scattered field and the Green's function in case of a dipole scatterer. Finally, expressions for the backscattering coefficients are derived in terms of the transverse spectral density of the scattered field.

2.1 PROBLEM FORMULATION

Consider the problem of scattering of time harmonic electromagnetic waves from discrete scatterers and the calculation of the backscattering coefficients from a slab of scatterers that are small compared to the wavelength of the incident field. It will be assumed that the density of scatterers ρ is constant. The physical configuration is shown in Fig. 2.1 which shows a three layer medium with free space above the vegetation layer of thickness 'd', and ground below it. The direction of the incoming wave vector $\bar{k}$, polarization vectors $\bar{h}^o$ or $\bar{v}^o$ and incident angle θ_o are as shown. The interface between the ground and the vegetation is assumed to be smooth.

Medium 0 is free space having permeability μ_o and permittivity ϵ_o. The scattering particles are all assumed to be identical and each has a volume V_p, relative dielectric constant ϵ_r and free space permeability μ_o. Medium 2 is the ground underlying the vegetation with relative dielectric constant ϵ_g and permeability μ_o.

To compute the scattered field using the distorted Born approximation, we must first calculate the mean field in the slab containing the scattering particles. The mean wave is computed by replacing the particles with an equivalent medium having relative permittivity $\bar{\bar{\epsilon}}_e$.

The equations satisfied by the mean field in a medium of sparsely distributed dielectric scatterers have been

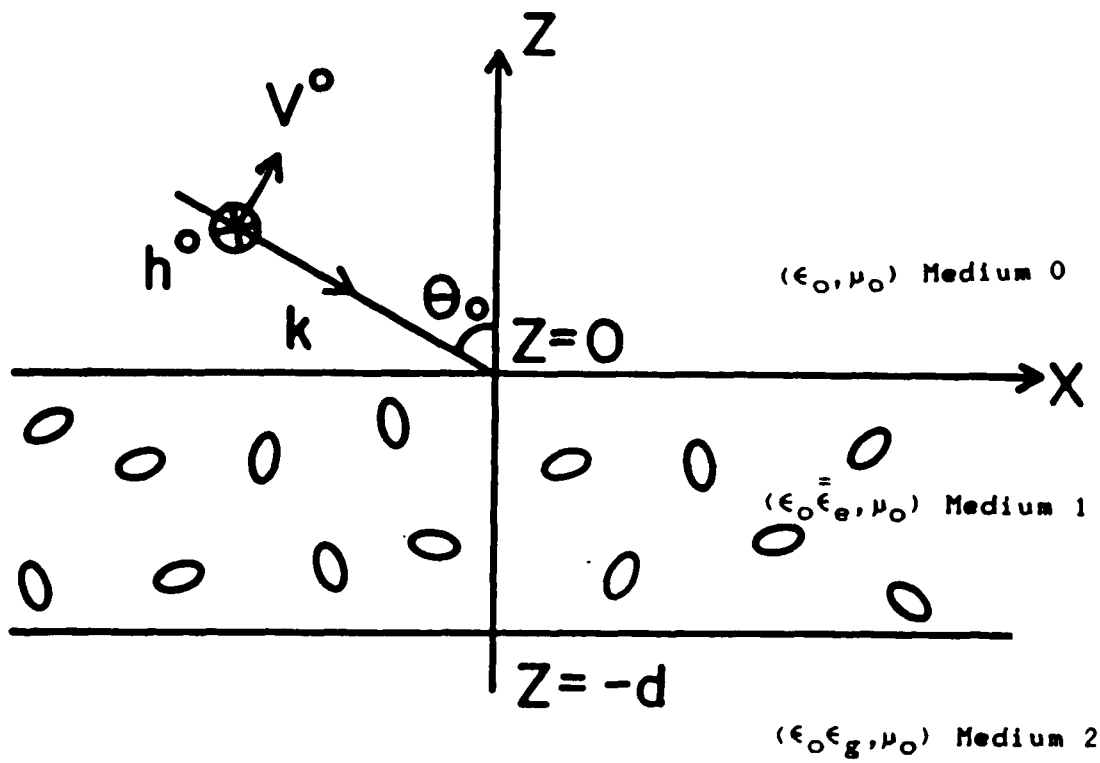

Fig. 2.1 Slab geometry with incident plane wave

derived by Lang[27]. There it was shown in the case of dipole scatterers that the average electric field, $\langle \bar{E}(\bar{x}) \rangle$, and the average magnetic field, $\langle \bar{H}(\bar{x}) \rangle$, obey Maxwells' equations

$$\nabla X \langle \bar{E}(\bar{x}) \rangle = i w \mu_o \langle \bar{H}(\bar{x}) \rangle \tag{2.1}$$

$$\nabla X \langle \bar{H}(\bar{x}) \rangle = i w \epsilon_o \bar{\bar{\epsilon}}_e(z) . \langle \bar{E}(\bar{x}) \rangle \tag{2.2}$$

in an equivalent medium having relative permeability 1 and relative permittivity $\bar{\bar{\epsilon}}_e(\bar{x})$. Here the relative permittivity $\bar{\bar{\epsilon}}_e(\bar{x})$ is a dyadic since the scatterers are arbitrarily shaped. The equivalent permittivity is represented as a sum of two terms,

$$\bar{\bar{\epsilon}}_e(z) = \bar{\bar{\epsilon}}^{(o)}(z) + \delta\bar{\bar{\epsilon}}^{(1)}(z) \tag{2.3}$$

where the first term is the permittivity of the background medium which is given by

$$\bar{\bar{\epsilon}}^{(o)}(z) = \begin{cases} \bar{\bar{I}} & z > -d \\ \epsilon_g \bar{\bar{I}} & z < -d \end{cases} \tag{2.4}$$

and where the second term is the contribution due to the dipole scatterers which is given by

$$\bar{\bar{\epsilon}}^{(1)}(z) = \begin{cases} \underline{\bar{\bar{a}}} & 0 > z > -d \\ 0 & \text{elsewhere} \end{cases} \tag{2.5}$$

In eq.(2.4), $\bar{\bar{I}}$ is the unit dyadic and in eq.(2.5) $\bar{\bar{a}}$ is polarizability of a dipole scatterer normalized to the scatterer's volume V_p. The bar under $\bar{\bar{a}}$ denotes the average over the scatterer's angular orientation variables Θ and $\emptyset$.

Thus we have

$$\bar{\bar{a}} = \int_0^{2\pi} d\phi \int_0^{\pi} d\theta \, P_\theta(\theta) P_\phi(\phi) \bar{\bar{a}}(\theta,\phi) \tag{2.6}$$

with $P_\theta(\theta)$ and $P_\phi(\phi)$ being the probability density functions of the orientation angles. The parameter δ appearing in eq.(2.3) is the fractional volume occupied by the particles. Therefore, it is the product of the particle density ρ and the particle volume V_p such that $\delta = \rho V_p$. For the sparse distributions being considered, $\delta << 1$. The fractional volume δ has been exhibited explicitly in eq.(2.3) since it will be employed as a perturbation parameter in the approximate calculation of the mean field.

To model the vegetative layer, only the effect of the leaves is considered. These are represented by lossy circular dielectric discs of radius 'a' and thickness 'h'. Since the leaves are usually distributed uniformly about the stem of the plant, we assume $P_\phi(\phi) = 1/2\pi$, $0 \leq \phi < 2\pi$. If the average indicated in eq.(2.6) is performed over ϕ, the average normalized polarizability $\bar{\bar{a}}$ becomes diagonal when expressed in Cartesian coordinates. Therefore,

$$\bar{\bar{a}} = a_{xx}\bar{x}^o\bar{x}^o + a_{yy}\bar{y}^o\bar{y}^o + a_{zz}\bar{z}^o\bar{z}^o \tag{2.7}$$

where

$$a_{xx} = a_{yy} = \overline{(a_r \sin^2\theta + a_\theta \cos^2\theta + a_\phi)} \tag{2.8}$$

and

$$a_{zz} = \overline{a_r \cos^2\theta + a_\theta \sin^2\theta} \tag{2.9}$$

The underbar expresses angular averaging with respect to θ. For circular discs,

$$a_r = \Delta/(1+\Delta) \tag{2.10}$$

and

$$a_\theta = a_\phi = \Delta \tag{2.11}$$

where $\Delta = \epsilon_r - 1$ is the difference between the dielectric constant of the disc and free space, and $V_p = \pi a^2 h$. Because all the off diagonal terms have averaged to zero and two of the on diagonal terms a_{xx} and a_{yy} are equal, the equivalent dielectric constant is uniaxial. This means that TE and TM waves do not couple at the level of the mean wave. Now knowing the equivalent dielectric constant in all regions, we can solve eqs.(2.1) and (2.2) with the proper boundary conditions to find the mean field in the equivalent medium. This mean field is determined in section 2.2.

The next step in determining the backscattering coefficients from the slab is to find the correlation function of the scattered field. The scattered field, $\bar{E}_s(\bar{x})$, is determined by Taylor[40], using the distorted Born approximation. Basically, this technique embeds the scatterers in the equivalent medium and then uses a single scattering approximation to determine the scattered field. It differs from the regular Born approximation in that the attenuation in the equivalent medium of the incident and scattered waves is taken into account. It is valid when the scattering albedo of an individual particle is small. Leaves in the frequency regime

below several GHz satisfy this criterion.

Following Lang[27], and employing the distorted Born approximation, we find that the correlation of the fluctuating component of the scattered field, $\bar{E}_f(\bar{x}) = \bar{E}_s(\bar{x}) - \langle \bar{E}_s(\bar{x}) \rangle$, is

$$\langle \bar{E}_f(\bar{x}) \bar{E}^*_f(\hat{\bar{x}}) \rangle = \int_V d\bar{s}\; p\; \overline{\bar{e}_{s_e}(\bar{x},\bar{s}) \bar{e}^*_{s_e}(\hat{\bar{x}},\bar{s})} \qquad (2.12)$$

where α^* denotes the complex conjugate of α, V is the volume of the slab of vegetation and $\bar{e}_{s_e}(\bar{x},\bar{s})$ is the scattered field at $\bar{x}$ due to a scatterer at $\bar{s}$. Thus we see that eq.(2.12) is just an incoherent addition of the contributions from individual scatterers. The overbar is the average over all scatterer orientations.

For the case of dipole scatterers, the expression for $\bar{e}_{s_e}$ is particularly simple. It is given by

$$\bar{e}_{s_e}(\bar{x},\bar{s}) = k_o^2 V_p \bar{\bar{G}}(\bar{x},\bar{s}) \cdot \bar{\bar{a}} \cdot \langle \bar{E}(\bar{s}) \rangle \qquad (2.13)$$

Here $\langle \bar{E}(\bar{s}) \rangle$ is the total mean field incident on the dipole scatterer located at $\bar{s}$ and having polarizability $\bar{\bar{a}}$. The function $\bar{\bar{G}}(\bar{x},\bar{s})$ is the Green's function that gives the scattered field at $\bar{x}$ in response to a unit dipole located at $\bar{s}$. The Green's function is calculated in the equivalent medium and thus is an averaged quantity. The correlation of the fluctuation field $\bar{E}_f(\bar{x})$ is calculated instead of the correlation of $\bar{E}_s(\bar{x})$ so that effects of specular reflection are eliminated from the backscatter coefficient expressions.

The backscattering coefficients are directly related

to the transverse Fourier transform of eq.(2.12) with respect to $\bar{x}_t$ and $\hat{\bar{x}}_t$ evaluated at the upper interface (z=0). Here the transverse vectors are defined as $\bar{x} = \bar{x}_t + z\bar{z}_o$ and $\hat{\bar{x}} = \hat{\bar{x}}_t + z\hat{\bar{z}}_o$ with $\bar{x}_t \cdot \bar{z}_o = \hat{\bar{x}}_t \cdot \hat{\bar{z}}_o = 0$. If we use the fact that the equivalent medium is translationally invariant in directions parallel to the slab interface, we have

$$\bar{\bar{G}}(\bar{x},\bar{s}) = \bar{\bar{G}}(\bar{x}_t - \bar{s}_t, z, s) \tag{2.14}$$

and

$$\bar{e}_{s_e}(\bar{x},\bar{s}) = \bar{e}_{s_e}(\bar{x}_t - \bar{s}_t, z, s) \tag{2.15}$$

with $\bar{s} = \bar{s}_t + s\bar{z}^o$.

Performing the indicated Fourier transform of eq.(2.12), integrating out $\bar{s}_t$ and evaluating the results at $z=\hat{z}=0$, we obtain

$$\langle \bar{E}_f(\bar{k}_t,0)\bar{E}_f^*(\hat{\bar{k}}_t,0)\rangle = \overline{\bar{\bar{S}}(\bar{k}_t,q)}\,\delta(\bar{k}_t - \hat{\bar{k}}_t) \tag{2.16}$$

where $\bar{A}(\bar{k}_t,z)$ is the transverse Fourier transform of $\bar{A}(\bar{x}_t,z)$ and

$$\bar{\bar{S}}(\bar{k}_t,q) = (2\pi)^2 \delta V_p \int_{-d}^{o} ds\; \bar{e}_{s_e}(\bar{k}_t,0,s)\bar{e}_{s_e}^*(\hat{\bar{k}}_t,0,s) \tag{2.17}$$

as defined by Lang[27], and

$$\bar{e}_{s_e}(\bar{k}_t,0,s) = k_o^2 V_p \bar{\bar{G}}(\bar{k}_t,0,s).\bar{\bar{a}}.\langle \bar{E}(\bar{s},q)\rangle \tag{2.18}$$

In eq.(2.16), $\bar{\bar{S}}(\bar{k}_t,q)$ is the transverse spectral density of $\bar{E}_f(x)$ at the interface and $\delta(\bar{k}_t)$ is the Dirac delta function.

If the mean field $\langle \bar{E}(\bar{s},q) \rangle$ used in eq.(2.18) is the response due to a plane wave of polarization $q \in \{h,v\}$ incident on the slab, then it is shown by Lang[27] that $\bar{\bar{S}}$ is directly related to the backscattering coefficients σ^o_{pq} by

$$\sigma^o_{pq} = \frac{k_o^2 \cos^2\theta_o}{4\pi^3} \bar{p}^o . \overline{\bar{\bar{S}}(-\bar{k}_{t_o},q)} . \bar{p}^o \qquad (2.19)$$

where θ_o is the angle of incidence of the plane wave with respect to the slab normal and $\bar{p}^o$. $\bar{p} \in \{\bar{h},\bar{v}\}$ is a unit vector indicating the polarization of the backscattered wave. We also have

$$\bar{k}_{t_o} = k_o \, \mathrm{Sin}\theta_o . \bar{x}^o \qquad (2.20)$$

Therefore, the knowledge of the mean field due to an incident plane wave and the Green's function in the equivalent medium can be used in conjunction with eqs.(2.17), (2.18) and (2.19) to determine the four backscattering cross sections σ^o_{hh} , σ^o_{hv} , σ^o_{vh} and σ^o_{vv} .

2.2 THE MEAN FIELD

In this section, we will find the mean wave in the equivalent medium for horizontal and vertical polarization cases. A plane wave is assumed to be incident at an angle θ_o as shown in Fig.2.2. Since the wave equation decomposes into horizontal and vertical modes, we will solve the horizontal case in detail and give the results for the vertical case. A two-variable perturbation procedure that takes advantage of the small parameter δ will be used to obtain approximate expressions for the mean field in both polarization cases.

The mean field is excited by a plane wave

$$\langle \bar{E}(\bar{x},q)\rangle = \bar{q}^o e^{i\bar{k}\cdot\bar{x}} \quad , \qquad q \in \{h,v_-\} \tag{2.21}$$

having polarization q. Here the wave vector is

$$\bar{k} = k_{x_o}\,\bar{x}^o + k_{z_o}\,\bar{z}^o \tag{2.22}$$

where, $k_{x_o} = k_o \sin\theta_o$ and $k_{z_o} = k_o \cos\theta_o$ (2.23)

and the polarization vectors are

$$\bar{h}^o = \bar{y}^o \qquad \text{, horizontal} \tag{2.24}$$

$$\bar{v}^o_{\pm} = \pm \cos\theta_o\,\bar{x}^o + \sin\theta_o\,\bar{z}^o \qquad \text{, vertical} \tag{2.25}$$

Because of the special dependence of the incident wave on $\bar{x}$ and the invariance of the mean equations in the x and y directions, we can write

$$\langle \bar{E}(\bar{x},q)\rangle = \langle \bar{E}(z,q)\rangle e^{ik x_o x} \tag{2.26}$$

$$\langle \bar{H}(\bar{x},q)\rangle = \langle \bar{H}(z,q)\rangle e^{ik x_o x} \tag{2.27}$$

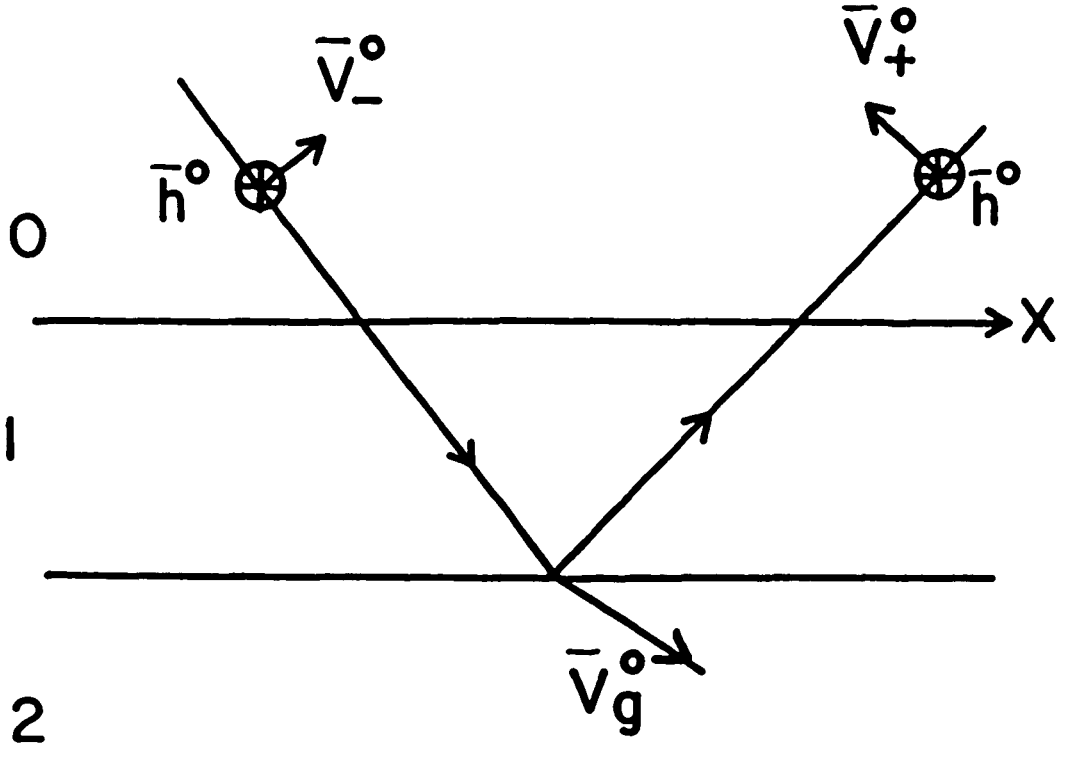

Fig. 2.2 Mean Wave Propagation

Substituting eqs.(2.26) and (2.27) into eqs.(2.1) and (2.2) and separating the ∇ operator into its longitudinal and transverse components, we can write,

$$(ik_{x_o}\bar{x}^o + \frac{d}{dz}\bar{z}^o) \times \langle\bar{E}(z,q)\rangle = i\omega\mu_o\langle\bar{H}(z,q)\rangle \qquad (2.28)$$

$$(ik_{x_o}\bar{x}^o + \frac{d}{dz}\bar{z}^o) \times \langle\bar{H}(z,q)\rangle = i\omega\epsilon_o\bar{\bar{\epsilon}}_e\langle\bar{E}(z,q)\rangle \qquad (2.29)$$

Taking the cross products in eq.(2.28) and eq.(2.29), and assuming no variation in the y direction, we can decompose these equations into horizontal ($\langle E_y\rangle,\langle H_x\rangle,\langle H_z\rangle$) and vertical ($\langle E_x\rangle,\langle E_z\rangle,\langle H_y\rangle$) polarization modes.

2.2.1 Horizontal Polarization

In this case, we will consider the incoming wave to be horizontally polarized. Eliminating $\langle H_x\rangle$ and $\langle H_z\rangle$ from eqs. (2.28) and (2.29), we obtain a single scalar wave equation for $\langle E_y\rangle$,

$$\left[\frac{d^2}{dz^2} + k_o^2\,\bar{\bar{\epsilon}}^{(o)}_{yy}(z) - k_{x_o}^2 + \delta k_o^2\,\bar{\bar{\epsilon}}^{(1)}_{yy}(z)\right]\langle E_y(z,h)\rangle = o \qquad (2.30)$$

where $\epsilon^{(i)}_{yy} = \bar{y}^o \cdot \bar{\bar{\epsilon}}^{(i)}(z) \cdot \bar{y}^o$, $\quad i = 0,1.$

The above differential equation can be solved along with the appropriate boundary conditions by using exact or approximate methods. If the exact solution is found, the presence of the small parameter δ will allow us to simplify it substantially. Physically, this results from the fact that for

small fractional volumes δ, the slab of vegetation has a dielectric constant close to that of free space. Thus interface effects at z=0 will be relatively unimportant. The most important effect will be the decay of mean wave due to the loss in the scatterers and the reflection from the ground.

The two-variable perturbation procedure will allow us to determine the approximate solution directly without having to find the more complicated exact solution first. A rigorous mathematical proof of this method is given in Smith[52]. Kevorkian and Cole[51] have applied this method under similar conditions. The idea of multi-variable method is to introduce several scaled variables directly into the intended approximation and then choose the dependence of the approximate solution on the variables so as to obtain a uniformaly valid approximation to the exact solution. In two-variable method we assume a fast variable z and a slow variable $\bar{z}=\delta z$ and consider $\langle E_y \rangle$ to be a function of z and $\bar{z}$. We have

$$\langle E_y(z) \rangle \equiv \Psi_y(z,\bar{z},\delta) = \sum_{n=0}^{\infty} \Psi_y^{(n)}(z,\bar{z})\delta^n \qquad (2.31)$$

and total derivative with respect to z can be written as a sum of partial derivatives,

$$\frac{d}{dz} = \frac{\partial}{\partial z} + \delta \frac{\partial}{\partial \bar{z}} \qquad (2.32)$$

Substituting eqs.(2.31) and (2.32) into eq.(2.30) we get,

$$\left[\left(\frac{\partial}{\partial z} + \delta \frac{\partial^2}{\partial \bar{z}}\right) + k_o^2 \epsilon_{yy}^{(o)}(z) - k_{x_o}^2 + \delta k_o^2 \epsilon_{yy}^{(1)}(z)\right] \sum_{n=o}^{\infty} \Psi_y^{(n)}(z,\bar{z})\delta = o \qquad (2.33)$$

By equating coefficients of δ, we find,

$$\delta^0: \quad \left[\frac{\partial^2}{\partial z^2} + k_o^2 \epsilon_{yy}^{(o)}(z) - k_{x_o}^2\right]\psi_y^{(o)}(z,\bar{z}) = 0 \tag{2.34}$$

$$\delta^1: \quad \left[\frac{\partial^2}{\partial z^2} + k_o^2 \epsilon_{yy}^{(o)}(z) - k_{x_o}^2\right]\psi_y^{(1)}(z,\bar{z}) =$$

$$-2\frac{\partial^2}{\partial z \partial \bar{z}}\psi_y^{(o)}(z,\bar{z}) - k_o^2 \epsilon_{yy}^{(1)}(z)\psi_y^{(o)}(z,\bar{z}) \tag{2.35}$$

The coefficients in the forcing function of eq.(2.35) will be selected such that no resonant terms will exist as explained later on, resulting in eqs.(2.43)-(2.45).

The solution to eq.(2.34) is considered first. The continuity of the electric and magnetic fields requires that $\psi_y^{(o)}$ and $\partial\psi_y^{(o)}/\partial z$ be continuous at z=0 and z=-d. The solution will be

$$\psi_y^{(o)}(z,\bar{z}) = \begin{cases} e^{-ik_{z_o}z} + r_o^{(h)}(\bar{z})e^{ik_{z_o}z} & ,z>0 \quad (2.36A) \\ T_o^{(h)}(\bar{z})e^{-ik_{z_o}z} + r_1^{(h)}(\bar{z})e^{ik_{z_o}z} & ,0>z>-d \quad (2.36B) \\ r_1^{(h)}(\bar{z})e^{-ik_{z_g}z} & ,z<-d \quad (2.36C) \end{cases}$$

where $k_{z_g} = \sqrt{k_o^2\epsilon_g - k_{x_o}^2}$. The coefficients $r_i^{(h)}(\bar{z})$, $T_i^{(h)}(\bar{z})$, i = 0,1 are assumed to be functions of the slow variable $\bar{z}$ and will be determined from the δ^1 equation. By using the continuity conditions at the z=0 and z=-d interface, we obtain

$$\Gamma_o^{(h)}(0) = 1 \tag{2.37}$$

$$\Gamma_o^{(h)}(0) = \Gamma_1^{(h)}(0) \tag{2.38}$$

$$T_o^{(h)}(-\bar{d}) = R_g^{(h)} e^{-2ik_{z_o}d}\, \Gamma_1^{(h)}(-\bar{d}) \tag{2.39}$$

$$T_1^{(h)}(-\bar{d}) = T_g^{(h)} e^{ik_{z_o}d}\, e^{-ik_{z_g}d} \tag{2.40}$$

where $\bar{d} = \delta d$

$$R_g^{(h)} = \frac{k_{z_o} - k_{z_g}}{k_{z_o} + k_{z_g}} \tag{2.41}$$

$$T_g^{(h)} = 1 + R_g^{(h)} \tag{2.42}$$

Now consider the next term in the perturbation series, $\psi_y^{(1)}(z,\bar{z})$. It satisfies eq.(2.35). The left hand side of this equation is the same as eq.(2.34), while the right hand side of the equation is a forcing term that depends on $\psi_y^{(o)}$. If any of the terms in the forcing function are resonant then the particular solution for $\psi_y^{(1)}$ will grow linearly in z and thus will not be bounded. The two-variable procedure eliminates these terms by choosing $\Gamma_1^{(h)}(\bar{z})$, $T_1^{(h)}(\bar{z})$ so the coefficients of the resonant terms are zero. We find

$$\frac{d}{d\bar{z}} \Gamma_o^{(h)}(\bar{z}) = 0 \qquad , \quad z>0 \tag{2.43}$$

$$2ik_{z_o} \frac{d}{d\bar{z}} \Gamma_1^{(h)}(\bar{z}) + k_o^2 \bar{a}_{yy} \Gamma_1^{(h)}(\bar{z}) = 0 \qquad , \quad 0>z>-d \tag{2.44A}$$

$$-2ik_{z_o} \frac{d}{d\bar{z}} T_o^{(h)}(\bar{z}) + k_o^2 \bar{a}_{yy} T_o^{(h)}(\bar{z}) = 0 \tag{2.44B}$$

and

$$\frac{d}{d\bar{z}} T_1^{(h)}(\bar{z}) = 0 \qquad , \quad z<-d \tag{2.45}$$

The above are first order differential equations involving reflection and transmission factors $r_o^{(h)}(\bar{z})$, $r_1^{(h)}(\bar{z})$, $T_o^{(h)}(\bar{z})$ and $T_1^{(h)}(\bar{z})$. Using eqs.(2.37)-(2.40) as the boundary values and solving eqs.(2.43)-(2.45), we get the following solution for the mean field,

$$\langle \bar{E}(z,h) \rangle \approx \bar{\bar{y}}_y^{(o)}(z,\bar{z})\bar{y}^o = \begin{cases} (e^{-ik_{z_o}z} + r_o^{(h)} e^{ik_{z_o}z})\bar{h}^o, & z>0 \quad (2.46A) \\ (e^{-ik_z^{(h)}z} + r_o^{(h)} e^{ik_z^{(h)}z})\bar{h}^o, & 0>z>-d \quad (2.46B) \\ (T_1^{(h)} e^{-ik_{z_g}z})\bar{h}^o, & z<-d \quad (2.46C) \end{cases}$$

where

$$r_o^{(h)} = R_g^{(h)} e^{2ik_z^{(h)}d} \qquad (2.47)$$

$$T_1^{(h)} = T_g^{(h)} e^{ik_z^{(h)}d} e^{-ik_{z_g}d} \qquad (2.48)$$

and

$$k_z^{(h)} = k_{z_o} + \frac{\delta k_o^2 \bar{\bar{a}}_{yy}}{2k_{z_o}} \qquad (2.49)$$

The Fresnel reflection and transmission coefficients for horizontal polarization $R_g^{(h)}$ and $T_g^{(h)}$ are defined in equations (2.41) and (2.42) respectively.

The first term in eq.(2.46A) is the incoming wave and the second term represents the reflected wave after travelling through the equivalent medium and having been reflected from underlying ground. The same is true inside the equivalent medium except that the propagation constant now is $k_z^{(h)}$, as defined by eq.(2.49). The original wave after decaying through the equivalent medium is partially transmitted

into the ground where it travels with a propagation constant k_{z_g}.

2.2.2 Vertical Polarization

Proceeding in a similar manner as in the case of horizontal polarization, and taking the incident wave to be $\bar{v}_-^o \exp(i\bar{k}.\bar{x})$, we again apply the two-variable procedure. The result is

$$\langle \bar{E}(z,v_-) \rangle = \begin{cases} \bar{v}_-^o e^{-ik_{z_o}z} + \bar{v}_+^o \Gamma_o^{(v)} e^{ik_{z_o}z} & ,z>0 \quad (2.50A) \\ \bar{v}_-^o e^{-ik_z^{(v)}z} + \bar{v}_+^o \Gamma_o^{(v)} e^{ik_z^{(v)}z} & ,0>z>-d \quad (2.50B) \\ \bar{v}_g^o T_1^{(v)} e^{-ik_{z_g}z} & ,z<-d \quad (2.50C) \end{cases}$$

where

$$\Gamma_o^{(v)} = R_g^{(v)} e^{2ik_z^{(v)}d} \quad (2.51)$$

$$T_1^{(v)} = T_g^{(v)} e^{ik_z^{(v)}d} e^{-ik_{z_g}d} \quad (2.52)$$

$$R_g^{(v)} = \frac{\epsilon_g k_{z_o} - k_{z_g}}{\epsilon_g k_{z_o} + k_{z_g}} \quad (2.53)$$

$$T_g^{(v)} = 1 + R_g^{(v)} \quad (2.54)$$

$$k_z^{(v)} = k_{z_o} + \frac{\delta k_o^2}{2k_{z_o}} (\bar{a}_{xx}\cos^2\theta_o + \bar{a}_{zz}\sin^2\theta_o) \quad (2.55)$$

and

$$\bar{v}_g^o = \frac{(\epsilon_g - \sin^2\theta_o)^{1/2}\,\bar{x}^o + \sin\theta_o\,\bar{z}^o}{(\epsilon_g)^{1/2}} \quad (2.56)$$

Finally, we will combine the vertical and horizontal polarization cases into a general expression:

$$\langle \bar{E}(z,q) \rangle = \begin{cases} e^{-ik_{z_o} z} \bar{q}_-^o + \Gamma_o^{(q)} e^{ik_{z_o} z} \bar{q}_+^o & ,z>0 \quad (2.57A) \\ e^{-ik_z^{(q)} z} \bar{q}_-^o + \Gamma_o^{(q)} e^{ik_z^{(q)} z} \bar{q}_+^o & ,0>z>-d \quad (2.57B) \\ T_1^{(q)} e^{-ik_{z_g} z} \bar{q}_g^o & ,z<-d \quad (2.57C) \end{cases}$$

where $q \in \{h,v\}$.

Here the unit polarization vectors in the horizontal case are in the same direction $\bar{h}_+^o = \bar{h}_-^o = \bar{h}_g^o = \bar{y}^o$.

CHAPTER 3

3.0 ELCTROMAGNETIC BACKSCATTERING COEFFICIENTS FROM A LAYER OF VEGETATION - SINGLE SCATTERING

When an electromagnetic wave travels in a medium containing many particles, the scattering behavior can be divided into two extreme cases: sparse and dense distributions. When the particle density is sparse, we can use a single scattering approximation. In this approximation, we assume that the incident wave from the source reaches the destination after encountering very few particles. The scattered wave is assumed to be due to a single scattering by a particle, and multiple scattering is assumed to be negligible. The dipole discrete scatterer technique is used to determine the backscattering coefficients in single scattering cases in this chapter. Multiple scattering effects are studied in Chapter 4 and Chapter 5 using Radiative Transfer approach.

3.1 BACKSCATTERING COEFFICIENTS

In this section, we calculate the horizontal, vertical and cross-polarized backscattering cross-sections from the layer of vegetation. To do this, we will employ the distorted Born approximation as discussed in section 2.1.

3.1.1 Calculation of σ^o_{vv}

By using eq.(2.19) with $p = v_-$ and $q = v_-$, we obtain

$$\sigma^o_{vv} = \frac{k_o^2 \cos^2\theta_o}{4\pi^3} [\bar{v}^o_- . \overline{\bar{\bar{S}}(-\bar{k}_{t_o}, v_-)} . \bar{v}^o_-] \qquad (3.1)$$

where the dyadic spectral density $\bar{\bar{S}}$ is given in terms of the mean field and the mean Green's function by eqs.(2.17) and (2.18). The mean field has been evaluated in section 2.2 and the Green's function is computed in Appendix A. In this appendix, the dyadic Green's function is computed by employing a procedure similar to the one used for the mean wave. In particular, the two-variable method is again used resulting in a zeroth-order solution for the Green's function. For the calculation of the backscattering coefficients, we require the Green's function with the observation point at z=0 and the source point at z_o=s. From eq.(A18) of Appendix A,

$$\bar{\bar{G}}(-\bar{k}_{t_o}, o, s) = -\frac{1}{2ik_o \cos\theta_o} [(e^{ik_z^{(h)} s} + r_o^{(h)} e^{-ik_z^{(h)} s}) \bar{h}^o \bar{h}^o + e^{ik_z^{(v)} s} \bar{v}^o_- \bar{v}^o_- + r_o^{(v)} e^{-ik_z^{(v)} s} \bar{v}^o_- \bar{v}^o_+] \qquad (3.2)$$

We proceed by dotting both sides of eq.(2.17) with $\bar{v}_-^o$ to obtain

$$\bar{v}_-^o \cdot \bar{\bar{S}}(-\bar{k}_{t_o}, v_-) \cdot \bar{v}_-^o = (2\pi)^2 \delta V_p \int_{-d}^{0} ds \, |\bar{v}_-^o \cdot \bar{e}_{s_e}(-\bar{k}_{t_o}, o, s)|^2 \qquad (3.3)$$

The expression under the integral sign in eq.(3.3) can be evaluated by using eq.(2.57) with q=v and eq.(3.2) in eq.(2.18). Therefore,

$$\bar{v}_-^o \cdot \bar{e}_{s_e}(-\bar{k}_{t_o}, o, s) = -\frac{1}{2ik_{z_o}} [\bar{v}_-^o \cdot \bar{\bar{a}} \cdot \bar{v}_-^o \, e^{2ik_z^{(v)} s} + \Gamma_o^{(v)} (\bar{v}_+^o \cdot \bar{\bar{a}} \cdot \bar{v}_-^o + \bar{v}_-^o \cdot \bar{\bar{a}} \cdot \bar{v}_+^o) + (\Gamma_o^{(v)})^2 \bar{v}_+^o \cdot \bar{\bar{a}} \cdot \bar{v}_+^o \, e^{-2ik_z^{(v)} s}] \qquad (3.4)$$

where

$$\bar{v}_\pm^o \cdot \bar{\bar{a}} \cdot \bar{v}_\pm^o \equiv a_{v_\pm v_\pm} = \cos^2\theta_o a_{xx} \mp \cos\theta_o \sin\theta_o (a_{xz} + a_{zx}) + \sin^2\theta_o a_{zz} \qquad (3.5)$$

$$\bar{v}_+^o \cdot \bar{\bar{a}} \cdot \bar{v}_-^o \equiv a_{v_+ v_-} = \bar{v}_-^o \cdot \bar{\bar{a}} \cdot \bar{v}_+^o \equiv a_{v_- v_+} = -\cos^2\theta_o a_{xx} + \sin^2\theta_o a_{zz} \qquad (3.6)$$

Now substituting eq.(3.4) into eq.(3.3), we see that there will be sixteen exponential integral terms to evaluate. Upon integration, nine of the terms are of lower order in δ due to phase cancellation and can be neglected. The remaining terms when averaged over all particle orientations give,

$$\sigma_{vv}^o = \sigma_{vvd}^o + \sigma_{vvdr}^o + \sigma_{vvr}^o \qquad (3.7)$$

where

$$\sigma^o_{vvd} = \frac{k_o^4 \delta V_p}{4\pi} \overline{|a_{v_-v_-}|^2} \left(\frac{1-e^{-4\,\mathrm{Im}k_z^{(v)}d}}{4\,\mathrm{Im}k_z^{(v)}}\right) \tag{3.8}$$

$$\sigma^o_{vvdr} = \frac{k_o^4 \delta V_p}{4\pi} 4\overline{|a_{v_-v_+}|^2} |r_o^{(v)}|^2 d \tag{3.9}$$

$$\sigma^o_{vvr} = \frac{k_o^4 \delta V_p}{4\pi} |r_o^{(v)}|^4 \overline{|a_{v_+v_+}|^2} \left(\frac{e^{4\,\mathrm{Im}k_z^{(v)}d}-1}{4\,\mathrm{Im}k_z^{(v)}}\right) \tag{3.10}$$

Here σ^o_{vvd} represents the direct backscattering contribution as shown in Fig. 3.1a. The incoming wave propagates into the vegetation and it is scattered directly back to the observer. When summed over all scatterers, eq.(3.8) results. The backscattering coefficient σ^o_{vvdr} as given by eq.(3.9) results from two different but similar mechanisms as shown in Fig. 3.1b. In one case, the wave is scattered and then reflected towards the observer, where as in the second case, the wave is first reflected from ground interface and then scattered towards the observer. Since both these mechanisms result in the same path length, both of these terms will interfere coherently, leading to a factor of 4 in eq.(3.9) instead of 2(for incoherent interference). The $|r_o^{(v)}|^2$ term represents single reflection from the ground interface.

The third term given by eq.(3.10) represents the sum of all waves which are first reflected from the ground, then scattered and then finally again reflected by the ground towards the observer as shown in Fig. 3.1c. The reflection coefficient $|r_o^{(v)}|^4$ appears in the equation since the wave in

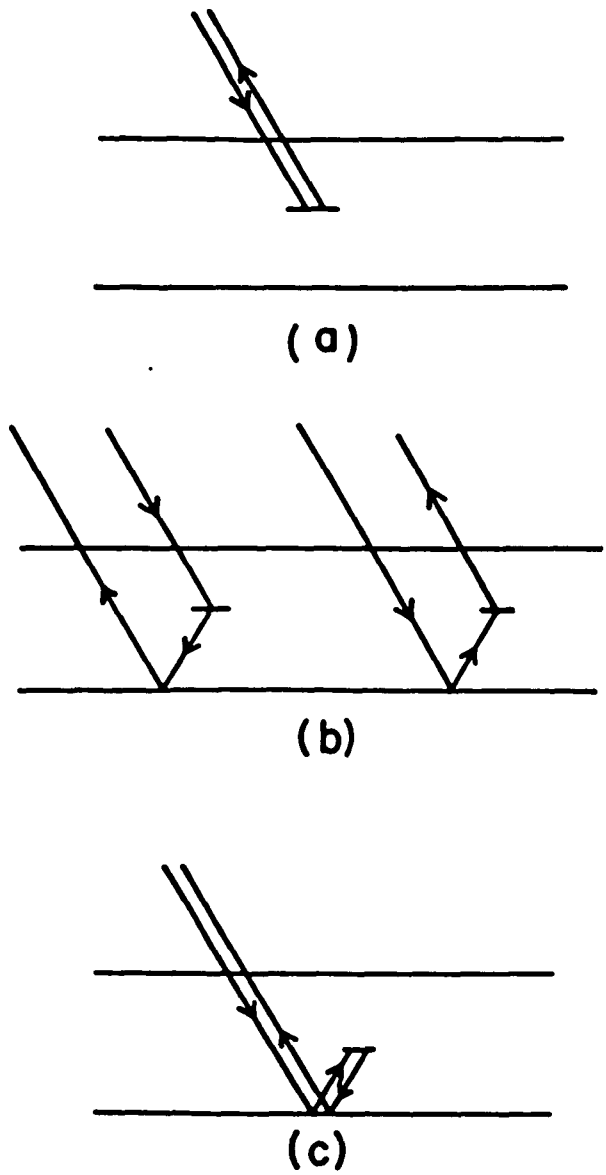

Fig. 3.1 Scattering Mechanisms

this case has been reflected by the ground twice.

The coefficients $\overline{|a_{v\_v\_}|^2}$, $\overline{|a_{v\_v+}|^2}$ and $\overline{|a_{v+v+}|^2}$ represents the average over θ and can be calculated from eqs.(3.5) and (3.6).

3.1.2 Calculation of σ^o_{hh}

Following the same procedure as in the case of σ^o_{vv}, we get

$$\sigma^o_{hh} = \sigma^o_{hhd} + \sigma^o_{hhdr} + \sigma^o_{hhr} \tag{3.11}$$

where

$$\sigma^o_{hhd} = \frac{k_o^4 \delta V_p}{4\pi} \overline{|a_{hh}|^2} \left(\frac{1-e^{-4\,\mathrm{Im}k_z^{(h)} d}}{4\,\mathrm{Im}k_z^{(h)}}\right) \tag{3.12}$$

$$\sigma^o_{hhdr} = \frac{k_o^4 \delta V_p}{4\pi} 4\overline{|a_{hh}|^2} |r_o^{(v)}|^2 d \tag{3.13}$$

$$\sigma^o_{hhr} = \frac{k_o^4 \delta V_p}{4\pi} |r_o^{(h)}|^4 \overline{|a_{hh}|^2} \left(\frac{e^{4\,\mathrm{Im}k_z^{(h)} d} - 1}{4\,\mathrm{Im}k_z^{(h)}}\right) \tag{3.14}$$

where $a_{hh} = a_{yy}$.

3.1.3 Calculation of σ^o_{vh} , σ^o_{hv}

In this case, incoming and reflected waves have different polarizations, thus the equation for σ^o_{vhdr} cannot be reduced to a simple term as in the previous two cases. But otherwise following a similar procedure we obtain

$$\sigma^o_{hv} = \sigma^o_{vh} = \sigma^o_{hvd} + \sigma^o_{hvdr} + \sigma^o_{hvr}$$

where

$$\sigma^o_{vhd} = \frac{k_o^4 \delta V_p}{4\pi} \overline{|a_{v\_h}|^2} \left[\frac{1-e^{-2\mathrm{Im}(k_z^{(v)}+k_z^{(h)})d}}{2\mathrm{Im}(k_z^{(v)}+k_z^{(h)})}\right] \tag{3.15}$$

$$\sigma^o_{vhdr} = \frac{k_o^4 \delta V_p}{4\pi} \{\overline{|a_{v+h}|^2} |r_o^{(v)}|^2 \left[\frac{1-e^{-2\mathrm{Im}(k_z^{(h)}-k_z^{(v)})d}}{2\mathrm{Im}(k_z^{(h)}-k_z^{(v)})}\right]$$

$$+ \overline{|a_{v\_h}|^2} |r_o^{(h)}|^2 \left[\frac{1-e^{-2\mathrm{Im}(k_z^{(v)}-k_z^{(h)})d}}{2\mathrm{Im}(k_z^{(v)}-k_z^{(h)})}\right]$$

$$. \overline{(a_{v+h} a^*_{v\_h})}\ 2\mathrm{Re}[r_o^{(v)} r_o^{(h)*} \frac{1-e^{-i2\mathrm{Re}(k_z^{(v)}-k_z^{(h)})d}}{i2\mathrm{Re}(k_z^{(v)}-k_z^{(h)})}]\} \tag{3.16}$$

$$\sigma^o_{vhr} = \frac{k_o^4 \delta V_p}{4\pi} \overline{|a_{v+h}|^2} |r_o^{(v)}|^2 |r_o^{(h)}|^2 \left[\frac{e^{2\mathrm{Im}(k_z^{(v)}+k_z^{(h)})d}-1}{2\mathrm{Im}(k_z^{(v)}+k_z^{(h)})}\right] \tag{3.17}$$

where,

$$a_{v\_h} = \cos\theta_o a_{xy} + \sin\theta_o a_{zy} \tag{3.18}$$

$$a_{v+h} = -\cos\theta_o a_{xy} + \sin\theta_o a_{zy} \tag{3.19}$$

and $\overline{|a_{v\_h}|^2}$, $\overline{|a_{v+h}|^2}$, $\overline{(a_{v+h} a^*_{v\_h})}$ represents the average over θ.

3.2 SKIN DEPTH

An examination of the expressions for the propagation constants $k_z^{(h)}$ and $k_z^{(v)}$ shows that since ϵ_r is complex, the Im $k_z^{(q)}$, $q \in \{h,v\}$ will be positive. Thus the mean wave decays as it propagates through the vegetation. Since the skin depth is given by the depth of penetration at which the wave's amplitude decreases to e^{-1} of its initial value, therefore,

$$\text{Skin Depth} = \frac{1}{\text{Im } k_z^{(q)}} \qquad q \in \{h,v\} \quad (3.20)$$

A knowledge of the skin depth will give us a better understanding of the mean wave's behavior inside the vegetation layer. We can see that if the vegetation depth is large compared to the skin depth, the effect of ground reflections will be negligible; whereas, when the skin depth is large compared to the layer thickness, the characteristics of the underlying ground become important in interpreting radar backscatter information.

Explicit expressions for the skin depth can be obtained by utilizing eqs.(2.49) and (2.55) in eq.(3.20) as follows,

$$\text{Skin Depth} = \begin{cases} \dfrac{2\,\text{Cos}\theta_o}{\delta k_o\ \text{Im}\ \underline{a}_{yy}} & \text{, h Polarization} \\ \dfrac{2\,\text{Cos}\theta_o}{\delta k_o(\text{Im}\ \underline{a}_{xx}\text{Cos}^2\theta_o + \text{Im}\ \underline{a}_{zz}\text{Sin}^2\theta_o)} & \text{,v Polarization} \end{cases} \quad (3.21)$$

where the average polarizability components, $\underline{a}_{xx}$, $\underline{a}_{yy}$ and $\underline{a}_{zz}$ are given in eqs.(2.8) and (2.9). Before computing the

skin depth, the dielectric constant of a leaf must be determined so that a_r, a_θ and a_ϕ can be determined from eqs.(2.10) and (2.11), and the distribution of leaves with respect to θ must be given. From Fung and Ulaby[11], who considered the leaf to be a mixture of water and solid material, the dielectric constant of a leaf can be calculated. For illustrative purposes, a mixture of 50% water and 50% solid material is chosen. At a frequency of 400 MHz this results in a dielectric constant of $\epsilon_r = 30.8+i0.62$. The following two angular distributions of leaves are considered,

$$P_{\theta_{\parallel}}(\theta) = \begin{cases} 1/\Delta\theta_{\parallel} & , \quad 0 \le \theta \le \Delta\theta_{\parallel} \\ 0 & , \quad \Delta\theta_{\parallel} < \theta \le \pi \end{cases} \tag{3.22}$$

and

$$P_{\theta_{\perp}}(\theta) = \begin{cases} 1/2\,\Delta\theta_{\perp} & , \quad \pi/2 - \Delta\theta_{\perp} \le \theta \le \pi/2 + \Delta\theta_{\perp} \\ 0 & , \quad \text{elsewhere} \end{cases} \tag{3.23}$$

The first distribution represents leaves that are approximately parallel to the vegetation interface when $\Delta\theta_{\parallel}$ is small and the leaves represented by the second distribution will be approximately perpendicular to the interface when $\Delta\theta_{\perp}$ is small.

In Figs.3.2 and 3.3, the skin depth as given in eq.(3.21) has been plotted as a function of the incident angle for both horizontal and vertical polarization at a frequency of 400 MHz. Fig. 3.2 is for a parallel distribution of leaves with

$\Delta\theta_{\parallel}=30^{o}$ while Fig. 3.3 is for a perpendicular distribution with $\Delta\theta_{\perp}=30^{o}$. An examination of eq.(3.2) shows that skin depth for both polarizations contains a factor of $\cos\theta_{o}$ in the numerator. This forces the skin depth to zero as the angle of incidence approaches grazing. This factor results from the fact that with increasing angle of incidence, the effective depth of propagation keeps decreasing for the same length of wave penetration.

Let us examine Fig. 3.2 in more detail. For horizontal polarization, the electric field is approximately parallel to the leaves at all angles of incidence and thus the skin depth has only a $\cos\theta_{o}$ dependence with θ_{o}. For vertical polarization on the other hand, the electric field is approximately parallel to the leaves for angles of incidence that are small. Thus it has the same skin depth in this angular region as the horizontal wave. As θ_{o} becomes larger, the electric field tends to become perpendicular to the leaves and thus less of the energy in the wave is lost in each leaf. This explains the increasing skin depth as a function of the angle of incidence for vertical polarization. Finally, the skin depth decreases in the vertical case due to the $\cos\theta_{o}$ in the numerator.

An examination of Fig. 3.3 shows that when the leaves have a perpendicular distribution, the horizontal skin depth is equal to or larger than the vertical skin depth. In this case, the electric field of the horizontally polarized wave is arbitrarily oriented with respect to a typical leaf. The electric field of the vertical wave has the same arbitrary

orientation at small angles of incidence. But as the angle of incidence increases, it becomes more nearly parallel to all leaves and thus has greater loss.

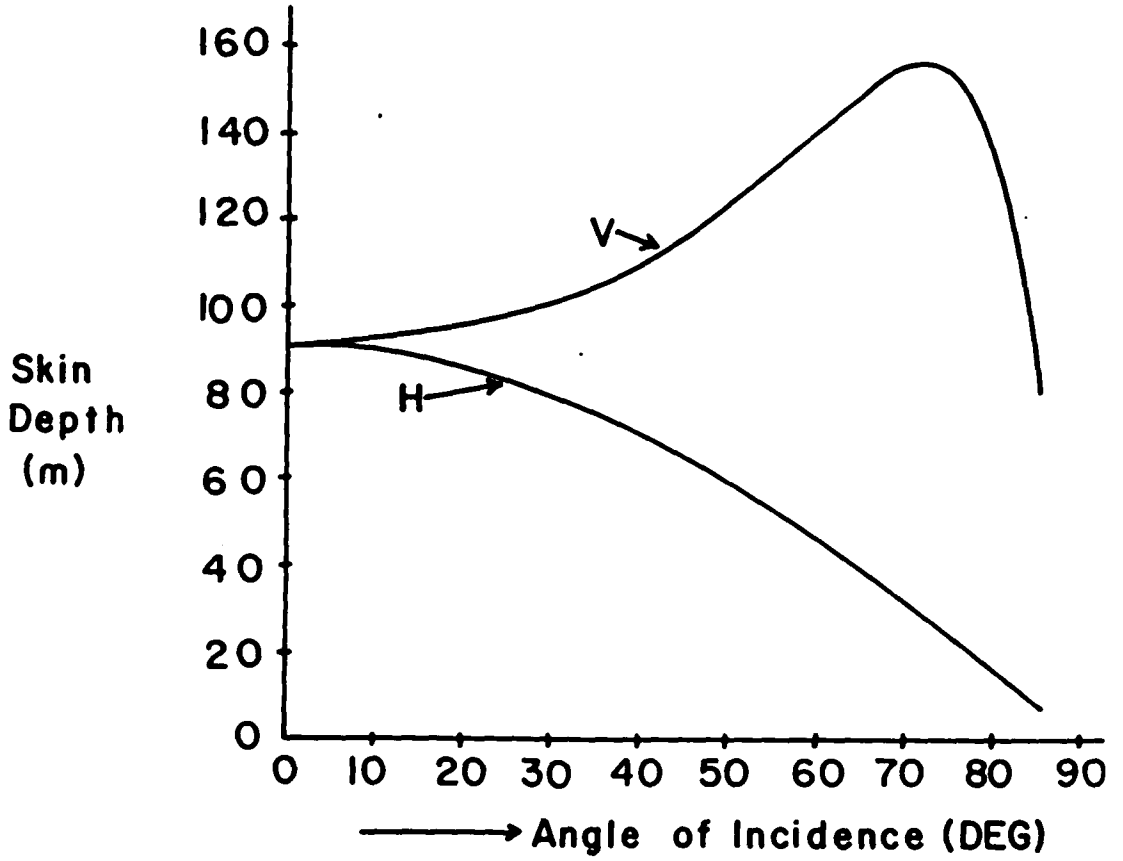

Fig. 3.1 Skin Depth vs. Angle of Incidence with $\Delta\theta_{II}=30°$, $\rho=500$, $f=400MHz$, $\varepsilon_r=30.8+i0.62$, $a=7.5cm$, and $h=0.5mm$.

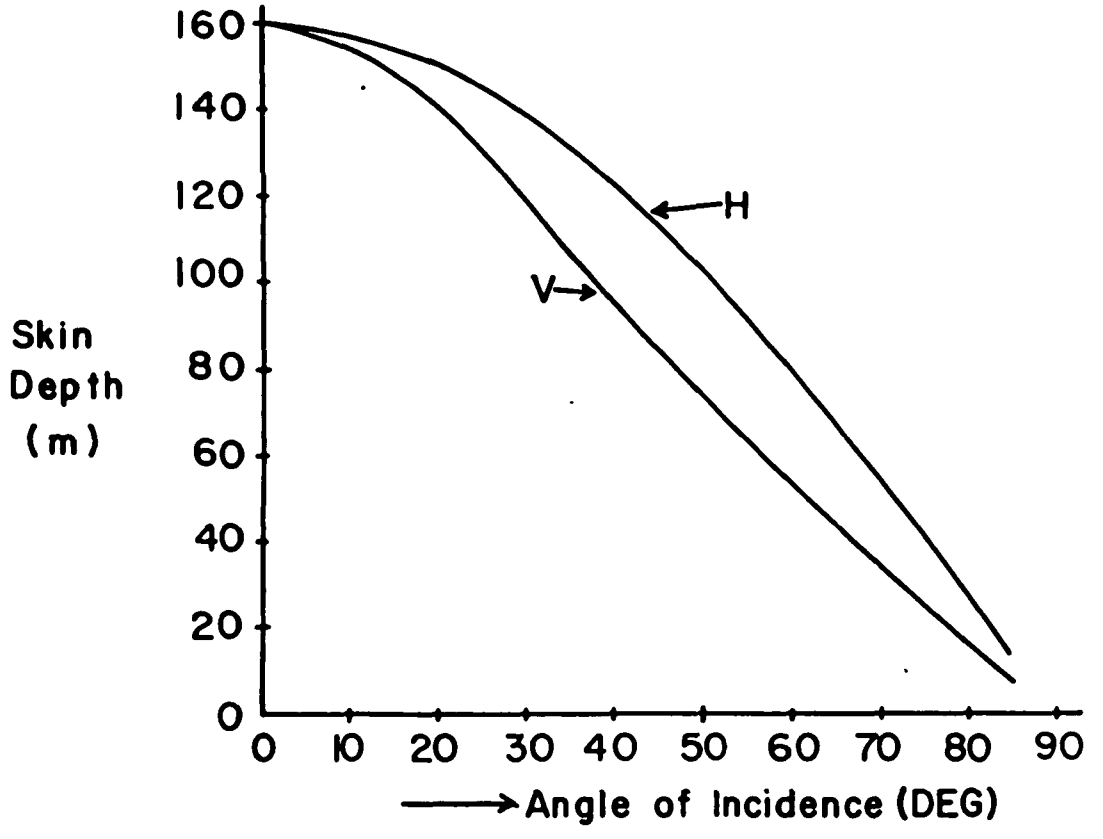

Fig. 3.3 Skin Depth vs. Angle of Incidence with $\Delta\theta_{\perp}=30°$, $\rho=500$, $f=400MHz$, $\epsilon_r=30.8+i0.62$, $a=7.5cm$, and $h=0.5mm$.

CHAPTER 4

4.0 RADIATIVE TRANSFER THEORY

Radiative Transfer Theory (RTT), also called Transport Theory, is capable of treating many physical phenomena. RTT deals directly with the transport of energy through a medium containing particles. It is assumed in RTT that there is no correlation between fields, and therefore, the addition of powers rather than the addition of fields holds.

In this chapter, the radiative transfer equations which govern the propagation of the intensities are derived for the homogeneous medium containing randomly distributed scatterers. The modified Stokes vector, the extinction matrix and the scattering matrix are defined. In RTT, the polarization effect is included through the Stokes vector. The total specific intensity is separated into reduced specific intensity and the diffused intensity. This results in a simple differential equation in terms of reduced intensity. A second equation relates the diffused intensity and the forcing function, due to the incident wave, in the form of a integro-differential equation.

The boundary condition at the upper and lower boundaries are derived by dividing the total intensity at any point into upward and downward travelling waves. A reflection coefficient matrix relating coupling between upward and downward travelling waves is defined.

Next, a Fourier series expansion in the azimuth direction is used to eliminate the Ø-dependence, resulting in independent radiative transfer equations. Similarly, the boundary conditions are also expanded in Fourier series in Ø. This results in sets of radiative transfer equations of different orders, with corresponding boundary conditions.

4.1 RADIATIVE TRANSFER EQUATIONS

The problem geometry is the same as shown in Fig. 2.1. The radiative transfer equation which governs the propagation of intensities inside the scattering medium is,

For $0 < \theta < \pi$,

$$\cos\theta \frac{d}{dz} \bar{I}(\theta,\phi,z) = - \bar{\bar{K}}(\theta).\bar{I}(\theta,\phi,z) + \int_0^{\pi} d\theta' \sin\theta' \int_0^{2\pi} d\phi' \bar{\bar{P}}(\theta,\phi,\theta',\phi').\bar{I}(\theta',\phi',z) \quad (4.1)$$

where $\bar{I}(\theta,\phi,z)$ is a four-component vector which represents the modified Stokes parameters as follows,

$$\bar{I}(\theta,\phi,z) = \begin{bmatrix} I_1(\theta,\phi,z) \\ I_2(\theta,\phi,z) \\ U(\theta,\phi,z) \\ V(\theta,\phi,z) \end{bmatrix} \quad (4.2)$$

$\bar{I}(\theta',\phi',z)$ is the incident intensity Stokes vector and $\bar{I}(\theta,\phi,z)$ represents the scattered intensity Stokes vector.

If all the particles are identical and oriented in the same direction, the scattering amplitude and therefore the scattering phase matrix is a deterministic function of θ,ϕ, θ',ϕ'. In general, the scatterers have size distributions and random orientations. Therefore, the extinction matrix and the phase matrix used in the radiative transfer equations should be the ensemble average of these quantities.

For a time harmonic field given by $\bar{E} = E_v \bar{v}^o + E_h \bar{h}^o$, where $\bar{v}^o$ and $\bar{h}^o$ represent two orthogonal polarizations (vertical and horizontal respectively), which are perpendicular to the propagation direction $\bar{k}$ as shown in Fig. 2.1 ($\bar{v}^o \times \bar{h}^o = \bar{k}$). The Stokes parameters are defined as:

$$I_1 = \langle |E_v|^2 \rangle \tag{4.3A}$$

$$I_2 = \langle |E_h|^2 \rangle \tag{4.3B}$$

$$U = 2\mathrm{Re}\langle E_v E_h^* \rangle \tag{4.3C}$$

$$V = 2\mathrm{Im}\langle E_v E_h^* \rangle \tag{4.3D}$$

where Re and Im denotes the real and imaginary parts respectively.

$\bar{\bar{P}}(\theta,\phi,\theta',\phi')$ is the scattering phase matrix and relates the scattered intensities in the θ,ϕ direction with the incident intensities from θ',ϕ' directions. The $\bar{\bar{P}}(\theta,\phi,\theta',\phi')$ matrix elements are defined as follows,

$$\bar{\bar{P}} = \rho \begin{bmatrix} \langle |f_{vv}|^2 \rangle & \langle |f_{vh}|^2 \rangle & \mathrm{Re}\langle f_{vv} f_{vh}^* \rangle & -\mathrm{Im}\langle f_{vv} f_{vh}^* \rangle \\ \langle |f_{hv}|^2 \rangle & \langle |f_{hh}|^2 \rangle & \mathrm{Re}\langle f_{hv} f_{hh}^* \rangle & -\mathrm{Im}\langle f_{hv} f_{hh}^* \rangle \\ 2\mathrm{Re}\langle f_{vv} f_{hv}^* \rangle & 2\mathrm{Re}\langle f_{vh} f_{hh}^* \rangle & \mathrm{Re}\langle f_{vv} f_{hh}^* + f_{vh} f_{hv}^* \rangle & -\mathrm{Im}\langle f_{vv} f_{hh}^* - f_{vh} f_{hv}^* \rangle \\ 2\mathrm{Im}\langle f_{vv} f_{hv}^* \rangle & 2\mathrm{Im}\langle f_{vh} f_{hh}^* \rangle & \mathrm{Im}\langle f_{vv} f_{hh}^* + f_{vh} f_{hv}^* \rangle & \mathrm{Re}\langle f_{vv} f_{hh}^* - f_{vh} f_{hv}^* \rangle \end{bmatrix} \tag{4.4}$$

ρ in the above equation is the number of particles per unit volume. If N(D) is the number of particles having sizes between D and D + ΔD, then

$$\rho = \int_0^\infty N(D)\,dD \tag{4.5}$$

$\bar{\bar{K}}(\theta)$ is the extinction matrix representing absorption and scattering losses, in the forward direction, and defined as follows,

$$\bar{\bar{K}} = \begin{bmatrix} 2\mathrm{Re}\ M_1 & 0 & \mathrm{Re}\ M_{12} & \mathrm{Im}\ M_{12} \\ 0 & 2\mathrm{Re}\ M_{22} & \mathrm{Re}\ M_{21} & -\mathrm{Im}\ M_{21} \\ 2\mathrm{Re}\ M_{21} & 2\mathrm{Re}\ M_{12} & \mathrm{Re}(M_{11}+M_{22}) & -\mathrm{Im}(M_{11}-M_{22}) \\ -2\mathrm{Im}\ M_{21} & 2\mathrm{Im}\ M_{12} & \mathrm{Im}(M_{11}-M_{22}) & \mathrm{Re}(M_{11}+M_{22}) \end{bmatrix} \tag{4.6}$$

where $M_{pq} = i\,\frac{2\pi}{k}\,\langle f_{pq}(\theta,\theta')\rangle \qquad p,q \in \{h,v\}$ (4.7)

and $f_{pq}(\theta,\theta')$ is the forward scattering amplitude ($\theta=\theta'$) averaged over the distribution of orientation and sizes of the scatterers. The derivations of scattering PHASE matrix and EXTINCTION matrix are described in Appendix B.

The total specific intensity $\bar{I}$ in eq.(4.1) can be divided into two components, the reduced incident intensity $\bar{I}_{ri}$ and the diffused intensity $\bar{I}_d$. As an incident wave enters the scattering volume, it decreases and increases according to the first and second terms in eq.(4.1) respectively. The part of the intensity that decreases due to scattering and

absorption, is called the reduced incident intensity and satisfies the following equation,

$$\mathrm{Cos}\theta \frac{d}{dz} \bar{I}_{ri}(\theta,\phi,z) = - \bar{\bar{K}}(\theta).\bar{I}_{ri}(\theta,\phi,z) \qquad (4.8)$$

The other part, which is created within the scattering volume because of multiple scattering, is called the diffuse intensity.

Substituting $\bar{I}(\theta,\phi,z) = \bar{I}_{ri}(\theta,\phi,z) + \bar{I}_{d}(\theta,\phi,z)$ in eq.(4.1), we get

$$\mathrm{Cos}\theta \frac{d}{dz} [\bar{I}_{d}(\theta,\phi,z)+\bar{I}_{ri}(\theta,\phi,z)] = - \bar{\bar{K}}(\theta).[\bar{I}_{d}(\theta,\phi,z)+\bar{I}_{ri}\theta,\phi,z)]$$

$$+ \int_{o}^{\pi} d\theta' \mathrm{Sin}\theta' \int_{o}^{2\pi} d\phi' \bar{\bar{P}}(\theta,\phi,\theta',\phi').[\bar{I}_{d}(\theta',\phi',z)+\bar{I}_{ri}(\theta',\phi',z)] \qquad (4.9)$$

Therefore, from eq.(4.8) and eq.(4.9), we get

$$\mathrm{Cos}\theta \frac{d}{dz} \bar{I}_{d}(\theta,\phi,z) = - \bar{\bar{K}}(\theta).\bar{I}_{d}(\theta,\phi,z)$$

$$+ \int_{o}^{\pi} d\theta' \mathrm{Sin}\theta' \int_{o}^{2\pi} d\phi' \bar{\bar{P}}(\theta,\phi,\theta',\phi').\bar{I}_{d}(\theta',\phi',z)+\bar{F}(\theta,\phi,\theta',\phi',z)$$

where

$$\bar{F}(\theta,\phi,\theta',\phi',z)=\int_{o}^{\pi} d\theta' \mathrm{Sin}\theta' \int_{o}^{2\pi} d\phi' \bar{\bar{P}}(\theta,\phi,\theta',\phi').\bar{I}_{ri}(\theta',\phi',z) \qquad (4.11)$$

is the equivalent source function generated by the reduced incident intensity.

4.1.1 Evaluating Source Function

In case of a plane wave incoming in the direction of θ_o, ϕ_o, we can represent it as a delta function. In a spherical coordinate system, we can write the reduced intensity as,

$$\bar{I}_{ri}(\theta,\phi,z) = [e^{-\bar{\bar{K}}(\theta).z\,Sec\theta}].\bar{I}_{oi}\,\delta(Cos\theta - Cos\theta_o)\,\delta(\phi-\phi_o) \qquad (4.12)$$

where $\bar{I}_{oi}$ is the intensity at z=0 in θ_o, ϕ_o direction. Substituting for $\bar{I}_{ri}(\theta,\phi,z)$ into eq.(4.11) and integrating over θ' and ϕ', we get

$$\bar{F}(\theta,\phi,\theta_o,\phi_o,z) = \bar{\bar{P}}(\theta,\phi,\theta_o,\phi_o).[e^{-\bar{\bar{K}}(\theta_o).z.Sec\theta_o}].\bar{I}_{oi} \qquad (4.13)$$

4.2 Boundary Conditions

As discussed in Chapter 2, since the dielectric constant inside the vegetation layer is close to that of the free space, any reflections at z = 0 interface will be neglected. Therefore, we have for $0 < \theta < \pi/2$,
at z = 0

For the downward travelling wave since their are no reflections at the interface,

$$\bar{I}(\pi-\theta,\phi,z=o^-) = \bar{I}_{oi}(\pi-\theta_o,\phi_o,z=o^+) \tag{4.14}$$

Decomposing the total intensity into reduced and diffused intensities, we can write,

$$\bar{I}_{ri}(\pi-\theta,\phi,z=o^-)+\bar{I}_d(\pi-\theta_o,\phi_o,z=o^-)=\bar{I}_{oi}(\pi-\theta_o,\phi_o,z=o^+) \tag{4.15}$$

Since the diffused intensity is generated inside the scattering material because of the multiple scattering, at the top interface,

$$\bar{I}_d(\pi-\theta,\phi,z=o^-) = 0 \tag{4.16}$$

Therefore, the wave entering the vegetation layer will be the unattenuated incoming wave such that,

$$\bar{I}_{ri}(\pi-\theta,\phi,z=o^-) = \bar{I}_{oi}(\pi-\theta_o,\phi_o,z=o^+) \tag{4.17}$$

Similarly, for the wave travelling in the upward

direction, since the reflections at the interface are unimportant, therefore the wave stays unchanged as it travels through the interface. Therefore for upward travelling wave,

$$\bar{I}(\theta,\emptyset,z=o^{+}) = \bar{I}(\theta,\emptyset,z=o^{-}) \tag{4.18}$$

Again decomposing the total intensity into the reduced and diffused intensities, we have,

$$\bar{I}_{ri}(\theta,\emptyset,z=o^{+}) = \bar{I}_{ri}(\theta,\emptyset,z=o^{-}) \tag{4.19}$$

and

$$\bar{I}_{d}(\theta,\emptyset,z=o^{+}) = \bar{I}_{d}(\theta,\emptyset,z=o^{-}) \tag{4.20}$$

at $z = -d$

The wave travelling downwards inside the vegetation layer is partially reflected at the ground interface and partially transmitted into the ground. Therefore,

$$\bar{I}(\theta,\emptyset,z=-d) = \bar{\bar{r}}(\theta)\bar{I}(\pi-\theta,\emptyset,z=-d) \tag{4.21}$$

Again decomposing into the reduced and diffused intensities, we have,

$$\bar{I}_{ri}(\theta,\emptyset,z=-d) = \bar{\bar{r}}(\theta)\bar{I}_{ri}(\pi-\theta,\emptyset,z=-d) \tag{4.22}$$

and

$$\bar{I}_{d}(\theta,\emptyset,z=-d) = \bar{\bar{r}}(\theta)\bar{I}_{d}(\pi-\theta,\emptyset,z=-d) \tag{4.23}$$

Here we have broken up total intensity in the scattering layer into upward going intensity $\bar{I}(\theta,\phi,z)$ and downward going intensity $\bar{I}(\pi-\theta,\phi,z)$. $\bar{\bar{r}}(\theta)$ in the above equation is the reflection coefficient matrix representing coupling from downward going intensity into upward going intensity at z = -d. The reflection matrix is defined as follows (Ref.Shin and Kong[37]):

$$\bar{\bar{r}}(\theta) = \begin{bmatrix} |S(\theta)|^2 & 0 & 0 & 0 \\ 0 & |R(\theta)|^2 & 0 & 0 \\ 0 & 0 & Re[S(\theta)R^*(\theta)] & -Im[S(\theta)R^*(\theta)] \\ 0 & 0 & Im[S(\theta)R^*(\theta)] & Re[S(\theta)R^*(\theta)] \end{bmatrix} \tag{4.24}$$

Where $R(\theta)$ and $S(\theta)$ are the TE and TM Fresnal reflection coefficients and given as follows,

$$R(\theta) = \frac{\cos\theta - (\epsilon_2/\epsilon_o - \sin^2\theta)^{1/2}}{\cos\theta + (\epsilon_2/\epsilon_o - \sin^2\theta)^{1/2}} \tag{4.25}$$

$$S(\theta) = \frac{\epsilon_2\cos\theta - (\epsilon_2/\epsilon_o - \sin^2\theta)^{1/2}}{\epsilon_2\cos\theta + (\epsilon_2/\epsilon_o - \sin^2\theta)^{1/2}} \tag{4.26}$$

4.3 FOURIER SERIES EXPANSION IN THE AZIMUTH DIRECTION

In a general case of non-spherical particles, all Fourier components are coupled to one another. But if the particles are spherical or if they are axially symmetric with the axis pointed in the Z-direction, then the extinction matrix $\overline{\overline{K}}$ becomes independent of ϕ and the phase matrix $\overline{\overline{P}}$ becomes a function of $\phi-\phi'$. In these cases, all the coupling among the Fourier components disappears, and the Fourier components of the radiative transfer equation become independent of one another. Then the equation for each component can be solved separately.

In case of a disc, the scattering amplitude function as derived in Appendix B is,

$$\overline{|f_{hh}(\bar{o},\bar{i})|^2} = \frac{k_o^4 |x|^2 T^2}{(4\pi)^2} \int_0^{\pi} d\theta\, p(\theta) \int_0^{2\pi} \frac{1}{2\pi} d\bar{\phi}\, |1-\cos(\phi_s-\phi_i)$$

$$+ \frac{x}{x+1} \sin^2\theta \cos\bar{\phi} \cos[\bar{\phi}-(\phi_s-\phi_i)]|^2 |S(\tau_t)|^2 \qquad (4.27)$$

where

$$x = \epsilon_{disc} - 1 \qquad (4.28)$$

T = disc thickness

θ and ϕ are disc orientation angles as shown in Fig. B.1 and

$$\bar{\phi} = \phi - \phi_i \qquad (4.29)$$

For a circular disc with cross-section 'a', the shape function is,

$$S(\tau_t) = \frac{a}{\tau} J_1(2\pi\tau a) \tag{4.30}$$

where,

$$\tau = \frac{k_o}{2\pi}\sqrt{\alpha^2 + \beta^2} \tag{4.31}$$

with

$$\alpha = \mathrm{Cos}\theta[\mathrm{Sin}\theta_i \mathrm{Sin}\bar{\phi} + \mathrm{Sin}\theta_s \mathrm{Sin}(\bar{\phi}-(\phi_s-\phi_i)) - \mathrm{Sin}\theta(\mathrm{Cos}\theta_i + \mathrm{Cos}\theta_s)] \tag{4.32A}$$

and

$$\beta = \mathrm{Sin}\theta_i \mathrm{Cos}\bar{\phi} + \mathrm{Sin}\theta_s \mathrm{Cos}(\bar{\phi}-(\phi_s-\phi_i)) \tag{4.32B}$$

From eq.(4.27), we see that $\overline{|f_{hh}(\bar{o},\bar{i})|^2}$ is a function of θ_i, θ_s and $(\phi_s-\phi_i)$ only. So we can write,

$$\overline{|f_{hh}(\bar{o},\bar{i})|^2} = P_{22}(\theta_i,\theta_s,\phi_s-\phi_i) \tag{4.33}$$

Similarly we can see that all the other elements of the phase matrix are also functions of θ_i, θ_s and $(\phi_s-\phi_i)$ only. Therefore in the case of circular disc scatterers, the radiative transfer eq.(4.10) becomes,

$$\mathrm{Cos}\theta \frac{d}{dz}\bar{I}_d(\theta,\phi,z) = -\bar{\bar{K}}(\theta).\bar{I}_d(\theta,\phi,z)$$

$$+ \int_0^{\pi} d\theta' \mathrm{Sin}\theta' \int_0^{2\pi} d\phi' \bar{\bar{P}}(\theta,\theta',\phi-\phi')\bar{I}_d(\theta',\phi',z) + \bar{F}(\theta,\theta',\phi-\phi',z) \tag{4.34}$$

Now using the Fourier-series expansion in the azimuth direction, we can write the Ø dependent terms as a summation series as follows:

$$\bar{I}_d(\theta,\phi,z) = \sum_m \bar{I}_{dm}(\theta,z)e^{im\phi} \tag{4.35}$$

$$\bar{I}_{ri}(\theta,\phi,z) = \sum_m \bar{I}_{rim}(\theta,z)e^{im\phi} \tag{4.36}$$

$$\bar{P}(\theta,\theta',\phi-\phi') = \sum_m \bar{P}_m(\theta,\theta')e^{im(\phi-\phi')} \tag{4.37}$$

and

$$\bar{F}(\theta,\theta_o,\phi-\phi_o,z) = \sum_m \bar{F}_m(\theta,\theta_o,z)e^{im(\phi-\phi_o)} \tag{4.38}$$

where

$$\bar{I}_{dm} = \bar{I}^*_{-dm}\ ,\ \bar{I}_{rim} = \bar{I}^*_{-rim}\ ,\ \bar{P}_m = \bar{P}^*_{-m} \text{ and } \bar{F}_m = \bar{F}^*_{-m}$$

Therefore from eq.(4.34), we get.

$$\cos\theta \frac{d}{dz}\sum_m \bar{I}_{dm}(\theta,z)e^{im\phi} = -\bar{K}(\theta).\sum_m \bar{I}_{dm}(\theta,z)e^{im\phi}$$

$$+ \int_o^{\pi} d\theta' \sin\theta' \int_o^{2\pi} d\phi' \sum_m \bar{P}_m(\theta,\theta')e^{im(\phi-\phi')} \sum_l \bar{I}_{dl}(\theta',z)e^{il\phi'}$$

$$+ \sum_m \bar{F}_m(\theta,\theta_o,z)e^{im(\phi-\phi')}$$

or

$$\cos\theta \frac{d}{dz}\sum_m \bar{I}_{dm}(\theta,z)e^{im\phi} = -\bar{K}(\theta).\sum_m \bar{I}_{dm}(\theta,z)e^{im\phi}$$

$$+ \int_o^{\pi} d\theta' \sin\theta' \sum_{m,l} \bar{P}_m(\theta,\theta')\ .\bar{I}_{dl}(\theta',z)e^{im\phi}.2\pi\delta_{ml}$$

$$+ \sum_m \bar{F}_m(\theta,\theta_o,z)e^{im(\phi-\phi_o)} \tag{4.39}$$

or

$$\cos\theta \frac{d}{dz} \bar{I}_{dm}(\theta,z) = -\bar{\bar{R}}(\theta).\bar{I}_{dm}(\theta,z) + 2\pi\int_0^{\pi} d\theta' \sin\theta' \bar{\bar{P}}_m(\theta,\theta').I_{dm}(\theta',z) + \bar{F}_m(\theta,\theta_o,z)e^{im\phi_o} \quad (4.40)$$

$$m = 0, \pm1, \pm2, \ldots\ldots$$

and from eq.(4.8), we get(for reduced intensity)

$$\cos\theta \frac{d}{dz} \sum_m \bar{I}_{rim}(\theta,z)e^{im\phi} = -\bar{\bar{R}}(\theta).\sum_m \bar{I}_{rim}(\theta,z)e^{im\phi}$$

$$\cos\theta \frac{d}{dz} \bar{I}_{rim}(\theta,z) = -\bar{\bar{R}}(\theta).\bar{I}_{rim}(\theta,z) \quad \text{for all } m \quad (4.41)$$

4.3.1 BOUNDARY CONDITIONS, FOURIER SERIES EXPANSION

Expanding the incident intensity into a Fourier series, we get

$$\bar{I}_{oi}\delta(\cos\theta-\cos\theta_o)\delta(\phi-\phi_o) = \bar{I}_{oi}\delta(\cos\theta-\cos\theta_o)\left[\frac{1}{2\pi} + \frac{1}{\pi}\sum_{\substack{m=-\infty \\ m\neq 0}}^{\infty} e^{im(\phi-\phi_o)}\right] \quad (4.42)$$

Substituting eqs.(4.35),(4.36) and (4.42) into the boundary conditions and collecting terms with the same azimuthal dependence, we obtain for $0 < \theta < \pi/2$,

at $z = 0$,

For the downward travelling wave,

$$\bar{I}_{dm}(\pi-\theta, z=o^-) = 0 \qquad \text{for all } m \qquad (4.43)$$

$$\bar{I}_{rio}(\pi-\theta, z=o^-) = \bar{I}_{oi}\,\delta(\cos\theta-\cos\theta_o)\frac{1}{2\pi} \qquad \text{for } m=o \qquad (4.44A)$$

$$\bar{I}_{rim}(\pi-\theta, z=o^-) = \bar{I}_{oi}\,\delta(\cos\theta-\cos\theta_o)\frac{1}{\pi}\; e^{-im\phi_o} \qquad \text{for } m>1 \text{ and } m<-1 \qquad (4.44B)$$

For the upward travelling wave,

$$\bar{I}_{dm}(\theta, z=o^+) = \bar{I}_{dm}(\theta, z=o^-) \qquad \text{for all } m \qquad (4.45)$$

and

$$\bar{I}_{rim}(\theta, z=o^+) = \bar{I}_{rim}(\theta, z=o^-) \qquad \text{for all } m \qquad (4.46)$$

at $z = -d$

$$\bar{I}_{dm}(\theta, z=-d) = \bar{\bar{r}}(\theta)\,\bar{I}_{dm}(\pi-\theta, z=-d) \qquad \text{for all } m \qquad (4.47)$$

and

$$\bar{I}_{rim}(\theta, z=-d) = \bar{\bar{r}}(\theta)\,\bar{I}_{rim}(\pi-\theta, z=-d) \qquad \text{for all } m \qquad (4.48)$$

CHAPTER 5

5.0 ELECTROMAGNETIC BACKSCATTERING COEFFICIENTS FROM A LAYER OF VEGETATION - MULTIPLE SCATTERING

The set of radiative transfer equations without the $\emptyset$ dependence, as derived in chapter 4, are solved using the method of Gaussian quadrature. In this method, the radiation field is divided into 2N streams in μ_i (i=±1, ±2, ...±N) directions. In Gauss's quadrature formula, the interval (-1,1) corresponding to integration from 0 to π, is divided according to the zeros (μ_j) of the Legendre polynomial, $P_m(\mu)$.

The Gauss's quadrature formula is superior to other quadrature formulas because, for a given 'm', it evaluates the integral exactly for all polynomials of degree less than 2m and not merely those of degree less than m. So the Gauss's formula is almost twice as accurate as any other quadrature formula using only m values of the function in that interval.

In the next section, the integrals in the radiative transfer equations are replaced by an appropriately weighted sum over 2N intervals. Then zero-order system of linear equations is solved by obtaining eigen-values and eigen-vectors and by matching the proper boundary conditions.

5.1 ZERO-ORDER SOLUTIONS

The zeroth-order radiative transfer equation can be written from eq.(4.40) as follows, for m = 0,

$$\mathrm{Cos}\theta \frac{d}{dz} \bar{I}_{do}(\theta,z) = - \bar{\bar{K}}(\theta).\bar{I}_{do}(\theta,z) + 2\pi\int_{o}^{\pi} d\theta' \mathrm{Sin}\theta' \, \bar{\bar{P}}_{o}(\theta,\theta').\bar{I}_{do}(\theta',z) + \bar{F}_{o}(\theta,\theta_{o},z) \qquad (5.1)$$

and from eq.(4.41),

$$\mathrm{Cos}\theta \frac{d}{dz} \bar{I}_{rio}(\theta,z) = - \bar{\bar{K}}(\theta).\bar{I}_{rio}(\theta,z) \qquad (5.2)$$

The corresponding zeroth-order boundary conditions as given by eqs.(4.43) and (4.44A) are,

at z = 0, for the downward travelling wave, we have

$$\bar{I}_{do}(\pi-\theta,z=o^{-}) = 0 \qquad (5.3A)$$

$$\bar{I}_{rio}(\pi-\theta,z=o^{-}) = \bar{I}_{oi}\delta(\mathrm{Cos}\theta-\mathrm{Cos}\theta_{o})\frac{1}{2\pi} \qquad (5.3B)$$

and for the upward travelling wave, from eqs.(4.45) and (4.46), we get

$$\bar{I}_{do}(\theta,z=o^{+}) = \bar{I}_{do}(\theta,z=o^{-}) \qquad (5.3C)$$

$$\bar{I}_{rio}(\theta,z=o^{+}) = \bar{I}_{rio}(\theta,z=o^{-}) \qquad (5.3D)$$

Similarly, from eqs.(4.47) and (4.48), for the upward travelling wave,

at $z = -d$

$$\bar{I}_{do}(\theta, z=-d) = \bar{\bar{r}}(\theta) . \bar{I}_{do}(\pi-\theta, z=-d) \tag{5.4A}$$

$$\bar{I}_{rio}(\theta, z=-d) = \bar{\bar{r}}(\theta) . \bar{I}_{rio}(\pi-\theta, z=-d) \tag{5.4B}$$

The substitution

$$\mu = \cos\theta \tag{5.5A}$$

and $\mu' = \mathrm{Cos}\theta'$ (5.5B)

such that,

$$d\mu = -\mathrm{Sin}\theta \, d\theta \tag{5.6A}$$

and $d\mu' = -\mathrm{Sin}\theta' d\theta'$ (5.6B)

is used.

Substituting in eqs. (5.1) through (5.4), we get

$$\mu \frac{d}{dz} \bar{I}_{do}(\mu, z) = - \bar{\bar{K}}(\mu) . \bar{I}_{do}(\mu, z) + 2\pi \int_{-1}^{+1} d\mu' \bar{\bar{P}}_o(\mu, \mu') . \bar{I}_{do}(\mu', z) + \bar{F}_o(\mu, \mu_o, z) \tag{5.7}$$

and

$$\mu \frac{d}{dz} \bar{I}_{rio}(\mu, z) = - \bar{\bar{K}}(\mu) . \bar{I}_{rio}(\mu, z) \tag{5.8}$$

The corresponding boundary conditions are,

at $z = 0$

$$\bar{I}_{do}(-\mu, z=o^-) = 0 \tag{5.9A}$$

$$\bar{I}_{rio}(-\mu, z=o^-) = \bar{I}_{oi}\delta(\mu-\mu_o)\frac{1}{2\pi} \tag{5.9B}$$

and

$$\bar{I}_{do}(\mu, z=o^+) = \bar{I}_{do}(\mu, z=o^-) \tag{5.9C}$$

$$\bar{I}_{rio}(\mu, z=o^+) = \bar{I}_{rio}(\mu, z=o^-) \tag{5.9D}$$

at $z = -d$

$$\bar{I}_{do}(\mu, z=-d) = \bar{\bar{r}}(\mu).\bar{I}_{do}(-\mu, z=-d) \tag{5.10A}$$

$$\bar{I}_{rio}(\mu, z=-d) = \bar{\bar{r}}(\mu).\bar{I}_{rio}(-\mu, z=-d) \tag{5.10B}$$

5.1.1 EVALUATING DIFFUSED INTENSITY $\bar{I}_{do}$

Using Gauss's Quadrature formula, we can replace the integral in eq.(5.7) by a summation series. At a finite number of 2N points, we get from eq.(5.7),

$$\mu_i \frac{d}{dz}\bar{I}_{do}(\mu_i, z) = -\bar{R}(\mu_i).\bar{I}_{do}(\mu_i, z) + 2\pi \sum_{j=-N}^{N} a_j \bar{P}_o(\mu_i, \mu_j).\bar{I}_{do}(\mu_j, z) + \bar{F}_o(\mu_i, \mu_o, z) \tag{5.11}$$

where

$$\bar{F}_o(\mu_i, \mu_o, z) = \bar{P}_o(\mu_i, \mu_o).[e^{-\bar{R}(\mu_o)z}.\frac{1}{\mu_o}].\bar{I}_{oin} \tag{5.12}$$

is the forcing function and $\mu_{-j} = -\mu_j$ (5.13)

and from equation (5.8), we get

$$\mu_i \frac{d}{dz} \bar{I}_{rio}(\mu_i, z) = - \bar{\bar{K}}(\mu_i) . \bar{I}_{rio}(\mu_i, z) \qquad (5.14)$$

for all i = N, N-1, ... 1, -1, ... -(N-1), -N.

We can write eq.(5.11) in matrix form as,

$$\frac{d}{dz} \begin{bmatrix} \bar{I}_{do}(\mu_N, z) \\ \bar{I}_{do}(\mu_{N-1}, z) \\ \vdots \\ \bar{I}_{do}(\mu_{-N}, z) \end{bmatrix} = - \begin{bmatrix} \frac{1}{\mu_N} \bar{\bar{K}}(\mu_N) & 0 & \cdots 0 \\ 0 & \frac{1}{\mu_{N-1}} \bar{\bar{K}}(\mu_{N-1}) & \cdots 0 \\ \vdots & \vdots & \vdots \\ 0 & 0 & \cdots \frac{1}{\mu_{-N}} \bar{\bar{K}}(\mu_{-N}) \end{bmatrix} \begin{bmatrix} \bar{I}_{do}(\mu_N, z) \\ \bar{I}_{do}(\mu_{N-1}, z) \\ \vdots \\ \bar{I}_{do}(\mu_{-N}, z) \end{bmatrix}$$

$$+2\pi \begin{bmatrix} \frac{a_{+N}}{\mu_{+N}} \bar{\bar{P}}_o(\mu_{+N}, \mu_{+N}) & \cdots & \frac{a_{-N}}{\mu_{+N}} \bar{\bar{P}}_o(\mu_{+N}, \mu_{-N}) \\ \frac{a_{+N}}{\mu_{N-1}} \bar{\bar{P}}_o(\mu_{N-1}, \mu_{+N}) & \cdots & \frac{a_{-N}}{\mu_{N-1}} \bar{\bar{P}}_o(\mu_{N-1}, \mu_{-N}) \\ \vdots & & \vdots \\ \frac{a_{+N}}{\mu_{-N}} \bar{\bar{P}}_o(\mu_{-N}, \mu_{+N}) & \cdots & \frac{a_{-N}}{\mu_{-N}} \bar{\bar{P}}_o(\mu_{-N}, \mu_{-N}) \end{bmatrix} \begin{bmatrix} \bar{I}_{do}(\mu_{+N}, z) \\ \bar{I}_{do}(\mu_{N-1}, z) \\ \vdots \\ \bar{I}_{do}(\mu_{-N}, z) \end{bmatrix}$$

$$+ \begin{bmatrix} \frac{1}{\mu_{+N}} \bar{F}_o(\mu_N, \mu_o, z) \\ \frac{1}{\mu_{N-1}} \bar{F}_o(\mu_{N-1}, \mu_o, z) \\ \vdots \\ \frac{1}{\mu_{-N}} \bar{F}_o(\mu_{-N}, \mu_o, z) \end{bmatrix} \tag{5.15}$$

or

$$\frac{d}{dz} \begin{bmatrix} \bar{I}_{do}(\mu_N, z) \\ \bar{I}_{do}(\mu_{N-1}, z) \\ \vdots \\ \bar{I}_{do}(\mu_{-N}, z) \end{bmatrix} + \begin{bmatrix} \bar{\bar{S}}(\mu_N, \mu_N) & \cdots\cdots\cdots & \bar{\bar{S}}(\mu_N, \mu_{-N}) \\ \cdot & \bar{\bar{S}}(\mu_{N-1}, \mu_{N-1}) & \cdots\cdots \\ \vdots & \vdots & \vdots \\ \bar{\bar{S}}(\mu_{-N}, \mu_N) & \cdots\cdots\cdots & \bar{\bar{S}}(\mu_{-N}, \mu_{-N}) \end{bmatrix} \begin{bmatrix} \bar{I}_{do}(\mu_N, z) \\ \bar{I}_{do}(\mu_{N-1}, z) \\ \vdots \\ \bar{I}_{do}(\mu_{-N}, z) \end{bmatrix}$$

$$= \begin{bmatrix} \frac{1}{\mu_{+N}} \bar{F}_o(\mu_N, \mu_o, z) \\ \frac{1}{\mu_{N-1}} \bar{F}_o(\mu_{N-1}, \mu_o, z) \\ \vdots \\ \frac{1}{\mu_{-N}} \bar{F}_o(\mu_{-N}, \mu_o, z) \end{bmatrix} \tag{5.16}$$

where,

$$\bar{\bar{S}}(\mu_i, \mu_j) = \frac{1}{\mu_i} [\, \bar{\bar{R}}(\mu_i) - 2\pi a_i \bar{\bar{P}}_o(\mu_i, \mu_j)\,] \quad \text{for } i = j \tag{5.17A}$$

and

$$\bar{\bar{S}}(\mu_i, \mu_j) = -\frac{1}{\mu_i} 2\pi a_j \bar{\bar{P}}_o(\mu_i, \mu_j) \quad \text{for } i \neq j \tag{5.17B}$$

In compact matrix form, we can write,

$$\frac{d}{dz}\left[\bar{I}_{do}\right] + \left[\bar{\bar{S}}\right]\left[\bar{I}_{do}\right] = \bar{B}_o \tag{5.18}$$

From eqs.(5.9) and (5.10), evaluating boundary conditions at $\mu = \mu_i$, we get

$$\bar{I}_{do}(-\mu_i,\ z=0) = 0 \tag{5.19A}$$

$$\bar{I}_{do}(\mu_i,\ z=0^+) = \bar{I}_{do}(\mu_i,\ z=0^-) \tag{5.19B}$$

and $$\bar{I}_{do}(\mu_i,\ z=-d) = \bar{\bar{r}}(\mu_i).\bar{I}_{do}(-\mu_i, z=-d) \tag{5.19C}$$

$$i = 1,2,.....N.$$

Eq.(5.18) is a linear first order differential equation, and its general solution is given by the sum of its complementary solution $\bar{I}_{co}(z)$ and particular solution $\bar{I}_{po}(z)$.

5.1.1.1 PARTICULAR SOLUTION

The particular solution is obtained as,

$$\bar{I}_{po}(z) = [\bar{\bar{S}} - \bar{\bar{U}}]^{-1}\ \bar{B}(\mu_o, z) \tag{5.20}$$

where $\bar{\bar{U}}$ is a 2N X 2N unit matrix.

5.1.1.2 COMPLEMENTARY SOLUTION

The complementary solution satisfies the homogeneous equation,

$$\frac{d}{dz}[\bar{I}_{co}] + [\bar{\bar{S}}][\bar{I}_{co}] = 0 \qquad (5.21)$$

Let, $\bar{I}_{co}(z) = \bar{\beta}\, e^{\lambda z}$ be the solution, and substituting in equation (5.21), we get,

$$[\lambda\bar{\bar{U}} + \bar{\bar{S}}]\bar{\beta} = 0 \qquad (5.22)$$

This becomes a matrix eigen-value problem and to obtain a non-zero solution, the determinant of the matrix $\lambda\bar{\bar{U}} + \bar{\bar{S}}$ must vanish, so

$$\lambda\bar{\bar{U}} + \bar{\bar{S}} = 0 \qquad (5.23)$$

The determinant is a polynomial in λ of degree 2N, and therefore there are 2N values of $\lambda = \lambda_n$, n = ±1, ±2,.....±N, satisfying eq.(5.22). These are the eigen-values and for each eigen-value λ_n, $\bar{\beta}_n$ is the corresponding eigen-vector.

The complementary solution $\bar{I}_{co}$ is then given by a linear combination of all eigen-vectors with arbitrary coefficients C_n as,

$$\bar{I}_{co}(z) = \sum_{n=-N}^{N} C_n\bar{\beta}_n e^{\lambda_n z} = \sum_{n=1}^{N} C_{+n}[\bar{\beta}_{+n}]e^{-\lambda_n z} + \sum_{n=1}^{N} C_{-n}[\bar{\beta}_{-n}]e^{+\lambda_n z} \qquad (5.24)$$

Let,

$$\bar{C}_{+n} = [C_1 \quad C_2 \quad \ldots\ldots\ldots\ldots \quad C_N]^T \qquad (5.25A)$$

$$\bar{C}_{-n} = [\underline{C}_1 \quad C_{-2} \quad \ldots\ldots\ldots\ldots \quad C_{-N}]^T \qquad (5.25B)$$

and

$$\bar{E}(z)=[\bar{\beta}_1 e^{\lambda_1 z} \quad \bar{\beta}_2 e^{\lambda_2 z} \quad \ldots\ldots\ldots\ldots \quad \bar{\beta}_N e^{\lambda_N z}] \qquad (5.26A)$$

$$\bar{F}(z)=[\bar{\beta}_{-1} e^{-\lambda_1 z} \quad \bar{\beta}_{-2} e^{-\lambda_2 z} \quad \ldots\ldots\ldots\ldots \quad \bar{\beta}_{-N} e^{-\lambda_N z}] \qquad (5.26B)$$

Therefore, we can write,

$$\bar{I}_{co}(z) = [\bar{E}(z)].[\bar{C}_{+n}] + [\bar{F}(z)].[\bar{C}_{-n}] \qquad (5.27)$$

Using matrix partitioning, we can write,

$$\begin{bmatrix} \bar{I}^{+}_{co}(z) \\ \bar{I}^{-}_{co}(z) \end{bmatrix} = \begin{bmatrix} \bar{E}^{+}(z) \\ \bar{E}^{-}(z) \end{bmatrix} [\bar{C}_{+n}] + \begin{bmatrix} \bar{F}^{+}(z) \\ \bar{F}^{-}(z) \end{bmatrix} [\bar{C}_{-n}] \qquad (5.28)$$

where, $\bar{I}^{+}_{co}(z)$ represents the upward going (positive z-axis) terms and $\bar{I}^{-}_{co}(z)$ are the downward going (negative z-axis) terms.

Now the $\bar{\beta}_n$ consists of the following components,

$$\bar{\beta}_n = \begin{bmatrix} \beta_{n(+N)} \\ \beta_{n(+N-1)} \\ \vdots \\ \beta_{n(1)} \\ \beta_{n(-1)} \\ \vdots \\ \beta_{n(-N)} \end{bmatrix} = \begin{bmatrix} \bar{\beta}_{n^+} \\ \bar{\beta}_{n^-} \end{bmatrix} \qquad (5.29)$$

where $\bar{\beta}_{n^+}$ represents positive N terms and $\bar{\beta}_{n^-}$ represents negative N terms. Therefore,

$$\bar{E}^{+}(z)=[(\bar{\beta}_{1^+})\ e^{\lambda_1 z} \quad (\bar{\beta}_{2^+})\ e^{\lambda_2 z} \ldots\ldots\ldots (\bar{\beta}_{N^+})\ e^{\lambda_N z}] \qquad (5.30A)$$

Similarly,

$$\bar{\bar{E}}^{-}(z)=[(\bar{\beta}_{1-})\ e^{\lambda_1 z}\quad (\bar{\beta}_{2-})\ e^{\lambda_2 z}\ \ldots\ldots\ (\bar{\beta}_{N-})\ e^{\lambda_N z}] \qquad (5.30B)$$

$$\bar{\bar{F}}^{+}(z)=[(\bar{\beta}_{-1+})\ e^{-\lambda_1 z}\quad (\bar{\beta}_{-2+})\ e^{-\lambda_2 z}\ \ldots\ldots\ (\bar{\beta}_{-N+})\ e^{-\lambda_N z}] \qquad (5.30C)$$

and

$$\bar{\bar{F}}^{-}(z)=[(\bar{\beta}_{-1-})\ e^{-\lambda_1 z}\quad (\bar{\beta}_{-2-})\ e^{-\lambda_2 z}\ \ldots\ldots\ (\bar{\beta}_{-N-})\ e^{-\lambda_N z}] \qquad (5.30D)$$

It follows that eq.(5.28) can be separated into the following two equations,

$$\bar{I}^{+}_{co}(z) = [\bar{\bar{E}}^{+}(z)].[\bar{C}_{+n}] + [\bar{\bar{F}}^{+}(z)].[\bar{C}_{-n}] \qquad (5.31A)$$

and

$$\bar{I}^{-}_{co}(z) = [\bar{\bar{E}}^{-}(z)].[\bar{C}_{+n}] + [\bar{\bar{F}}^{-}(z)].[\bar{C}_{-n}] \qquad (5.31B)$$

5.1.1.3 TOTAL SOLUTION FOR DIFFUSED INTENSITY

The total solution for the diffused intensity is,

$$\bar{I}_{do}(z) = \bar{I}_{co}(z) + \bar{I}_{po}(z) \qquad (5.32)$$

So from eqs.(5.20) and (5.28), we get

$$\bar{I}^{+}_{do}(z) = [\bar{\bar{E}}^{+}(z)].[\bar{C}_{+n}] + [\bar{\bar{F}}^{+}(z)].[\bar{C}_{-n}] + \bar{I}^{+}_{p}(z) \qquad (5.33A)$$

and

$$\bar{I}^{-}_{do}(z) = [\bar{\bar{E}}^{-}(z)].[\bar{C}_{+n}] + [\bar{\bar{F}}^{-}(z)].[\bar{C}_{-n}] + \bar{I}^{-}_{p}(z) \qquad (5.33B)$$

Using the boundary conditions (5.19A) at z=0, and (5.19C) at z = -d, we get,

$$\bar{I}^{-}_{do}(0) = [\bar{\bar{E}}^{-}(0)].[\bar{C}_{+n}]+[\bar{\bar{F}}^{-}(0)].[\bar{C}_{-n}]+\bar{I}^{-}_{p}(0) = 0 \quad (5.34A)$$

and

$$[\bar{\bar{E}}^{+}(-d)].[\bar{C}_{+n}] + [\bar{\bar{F}}^{+}(-d)].[\bar{C}_{-n}] + \bar{I}^{+}_{po}(-d)$$

$$= \bar{\bar{r}}.([\bar{\bar{E}}^{-}(-d)].[\bar{C}_{+n}] + [\bar{\bar{F}}^{-}(-d)].[\bar{C}_{-n}] + \bar{I}^{-}_{po}(-d))$$

or

$$[\bar{\bar{E}}^{+}(-d)-\bar{\bar{r}}.\bar{\bar{E}}^{-}(-d)]\bar{C}_{+n} + [\bar{\bar{F}}^{+}(-d)-\bar{\bar{r}}.\bar{\bar{F}}^{-}(-d)]\bar{C}_{-n}$$

$$+ [\bar{I}^{+}_{po}(-d)-\bar{\bar{r}}.\bar{I}^{-}_{p}(-d)] = 0 \quad (5.34B)$$

Combining (5.34A) and (5.34B), we get

$$\begin{bmatrix} \bar{\bar{E}}^{-}(0) & \bar{\bar{F}}^{-}(0) & \bar{C}_{+n} \\ \bar{\bar{E}}^{+}(-d)-\bar{\bar{r}}.\bar{\bar{E}}^{-}(-d) & \bar{\bar{F}}^{+}(-d)-\bar{\bar{r}}.\bar{\bar{F}}^{-}(-d) & \bar{C}_{-n} \end{bmatrix} = -\begin{bmatrix} \bar{I}^{-}_{po}(0) \\ \bar{I}^{+}_{po}(-d)-\bar{\bar{r}}.\bar{I}^{-}_{p}(-d) \end{bmatrix}$$

(5.35)

This results in a set of 2n equations with 2n variables C_n. Solving this set of linear equations and substituting the results in eqs.(5.33A) and (5.33B) gives the total diffused intensities in positive and negative going directions respectively.

5.2 BACKSCATTERING COEFFICIENTS

The bistatic scattering coefficient $\tau_{\beta\alpha}(\theta,\phi,\theta',\phi')$ is defined as the ratio of the scattered power of polarization β per unit solid angle in the direction θ,ϕ and the intercepted incident power of polarization α in the direction θ',ϕ' averaged over 4π radians. Therefore,

$$\tau_{\beta\alpha}(\theta,\phi,\theta',\phi') = 4\pi \frac{\cos\theta . \bar{I}_{o\beta s}(\theta,\phi)}{\cos\theta' . \bar{I}_{o\alpha i}} \qquad (5.36)$$

where $\alpha,\beta \in \{h,v\}$

In backscattering direction, $\theta = \theta'$ and $\phi = \phi' + \pi$. Therefore the backscattering cross section per unit area is,

$$\sigma_{\beta\alpha}(\theta') = \cos\theta' . \tau_{\beta\alpha}(\theta',\phi'+\pi,\theta',\phi') \qquad (5.37)$$

5.2.1 HH CASE

When incident and scattered waves are horizontally polarized, we have,

$$\sigma_{HH}(\theta') = \cos\theta' . 4\pi \frac{\cos\theta' . \bar{I}_{oHs}(\theta',\phi'+\pi)}{\cos\theta' . \bar{I}_{oHi}}$$

or

$$\sigma_{HH}(\theta') = 4\pi \cos\theta' \frac{\bar{I}_{oHs}(\theta',\phi'+\pi)}{\bar{I}_{oHi}} \qquad (5.38)$$

5.2.2 VV CASE

Similarly, for the vertical polarization case,

$$\sigma_{VV}(\theta') = 4\pi \cos\theta' \frac{\bar{I}_{oVs}(\theta', \phi'+\pi)}{\bar{I}_{oVi}} \tag{5.39}$$

5.2.3 HV CASE

In the case where the incident wave is horizontally polarized and the scattered wave is vertically polarized, we have

$$\sigma_{HV}(\theta') = 4\pi \cos\theta' \frac{\bar{I}_{oVs}(\theta', \phi'+\pi)}{\bar{I}_{oHi}} \tag{5.40}$$

5.2.4 VH CASE

Similarly, for the case where the incident wave is vertically polarized and the scattered wave is horizontally polarized we have,

$$\sigma_{VH}(\theta') = 4\pi \cos\theta' \frac{\bar{I}_{oHs}(\theta', \phi'+\pi)}{\bar{I}_{oVi}} \tag{5.41}$$

As shown in section B.6, since the scattering phase matrix has the reciprocity property, 'H' and 'V' in eqs.(5.40) and (5.41) are interchangable, therefore,

$$\sigma_{VH}(\theta') = \sigma_{HV}(\theta') \tag{5.42}$$

6.0 DISCUSSION OF SINGLE AND MULTIPLE SCATTERING RESULTS AND COMPARISON WITH EXPERIMENTAL DATA

In this chapter, the numerical results for the backscattering coefficients are computed by modelling the vegetation by a layer of leaves. Before computing the backscattering cross sections as a function of incidence angle, the dielectric constant and the angular distribution of leaves is required. As discussed in Section 3.2, a dielectric constant of $\epsilon_r = 30.8 + i0.62$ will be used for leaves at 400 MHz. In addition, the angular distributions given by eqs.(3.22) and (3.23) will be used for parallel and perpendicular orientations of leaves respectively.

The numerical results for the skin depth have already been discussed in section 3.2, but the effects of skin depth on the backscattering cross sections will be examined here. Before examining the backscattering cross section results, the effects of frequency on the dielectric constant of a leave will be studied. From Fung and Ulaby[11], the relationships for the real and imaginary parts of the dielectric permittivity are,

$$\epsilon_r' = 5.5 + \frac{\epsilon_m - 5.5}{1+(f\tau)^2} \tag{6.1}$$

$$\epsilon_r'' = (\epsilon_m - 5.5)\ \frac{f}{1+(f\tau)^2} \tag{6.2}$$

where f is the frequency and τ is the relaxation time of the water content. The relaxation time depends on the temperature

and at 20^{o} C, $f\tau$ is approximately equal to $1.85/\lambda$, where λ is the free space wavelength in centimeters. The permittivity, ϵ_m, is the relative macroscopic static permittivity of a leaf and is given by,

$$\epsilon_m = 5 + 51.56V_m \tag{6.3}$$

where V_m is the volume filling factor and is selected to be 0.5 in this model.

Examining eq.(6.1) for the real part of dielectric constant we see that at small frequencies, ϵ_r' is approximately equal to ϵ_m and constant until 1GHz, but starts to decrease monotonically thereafter. The imaginary part is very small at low frequencies but start to increase linearly and reaches its maximum around 15 GHz. Thereafter it will decrease as an inverse function of the frequency. Changing the water content in the leaves will change ϵ_m, resulting in level change for real and imaginary parts, but will not change the overall shape of the functions.

6.1 SINGLE SCATTERING

Using the expressions derived in eqs.(3.7) through (3.19), the numerical results are presented in Fig. 6.1 through Fig. 6.6, where the backscattering coefficients are plotted as a function of the angle of incidence θ_o. The angular distribution given by eq.(3.22) with $\Delta\theta_{\parallel} = 10^{o}$ is used in Fig. 6.1 through Fig. 6.5 and the angular distribution given by eq.(3.23) with $\Delta\theta_{\perp} = 10^{o}$ is used in Fig. 6.6.

6.1.1 EFFECTS OF LAYER THICKNESS ON BACKSCATTERING COEFFICIETS

In Fig. 6.1, σ^{o}_{hhd}, σ^{o}_{hhdr} and σ^{o}_{hhr} are shown as function of θ_o. In this case, the term σ^{o}_{hhdr} is greater than σ^{o}_{hhd} for all angles of incidence. This means that the energy backscattered from the ground is a significant part of the total backscattered energy and should not be neglected. Since the skin depth is large compared to the layer thickness for all angles of incidence, we are receiving scattering back from the same number of scatterers for each angle of incidence, resulting in a flat behavior for σ^{o}_{hhd}. The reflected terms σ^{o}_{hhdr} and σ^{o}_{hhr} slopes up with increasing angle of incidence since the reflection constant $|r_h|$ is increasing as shown in the figure.

In Fig. 6.2, the backscattering coefficients are plotted for a layer of thickness d=100m. The results are quite different in this case since the total backscattering coefficient is basically due to the direct term σ^{o}_{hhd}. Contributions from the other two terms are very small because the incoming wave gets attenuated by the time it reaches the ground interface. A plot for skin depth vs. angle of incidence is also shown in Fig. 6.2, explaining the decreasing nature of σ^{o}_{hhdr} and σ^{o}_{hhr} terms. So it can be concluded in this case that the underlying ground is not very important.

Fig. 6.3 represents the backscattering cross section for different values of 'd'. The transition that the backscatter-

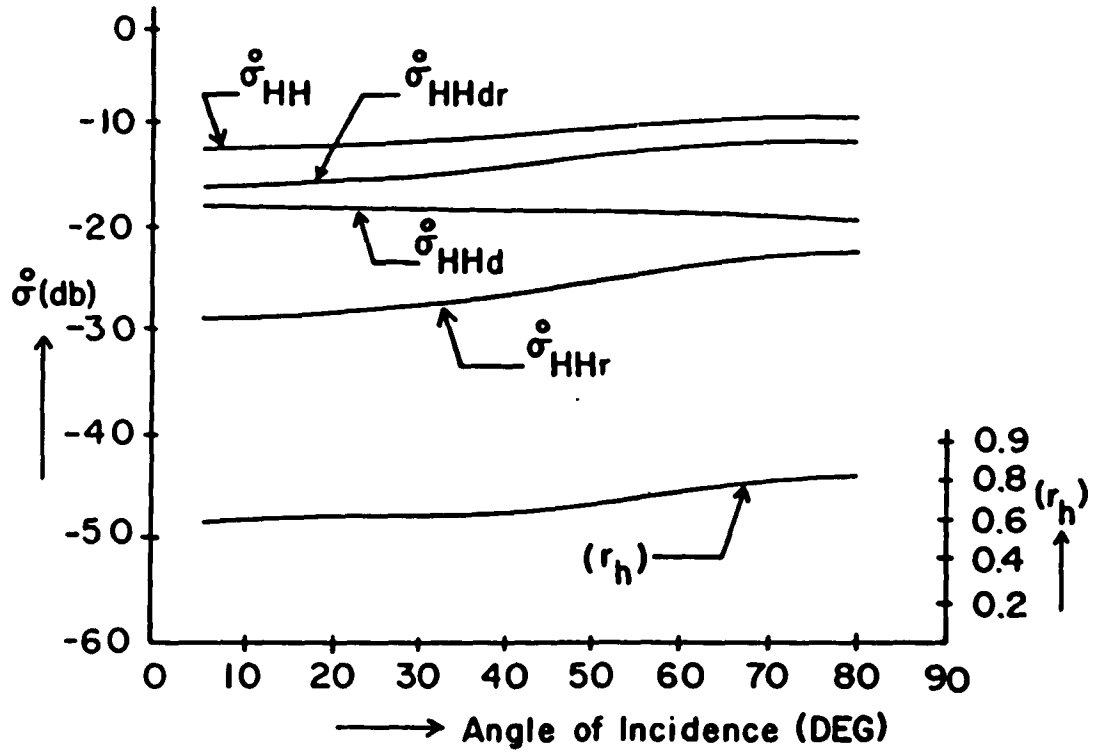

Fig. 6.1 Horizontal Copolarized Backscattering Cross Sections vs. Angle of Incidence with d=1m, $\Delta\theta_{if}$=10°, ρ=500, f=400MHz, ε_r=30.8+i0.62, ε_g=12+i3, a=7.5cm, and h=0.5mm.

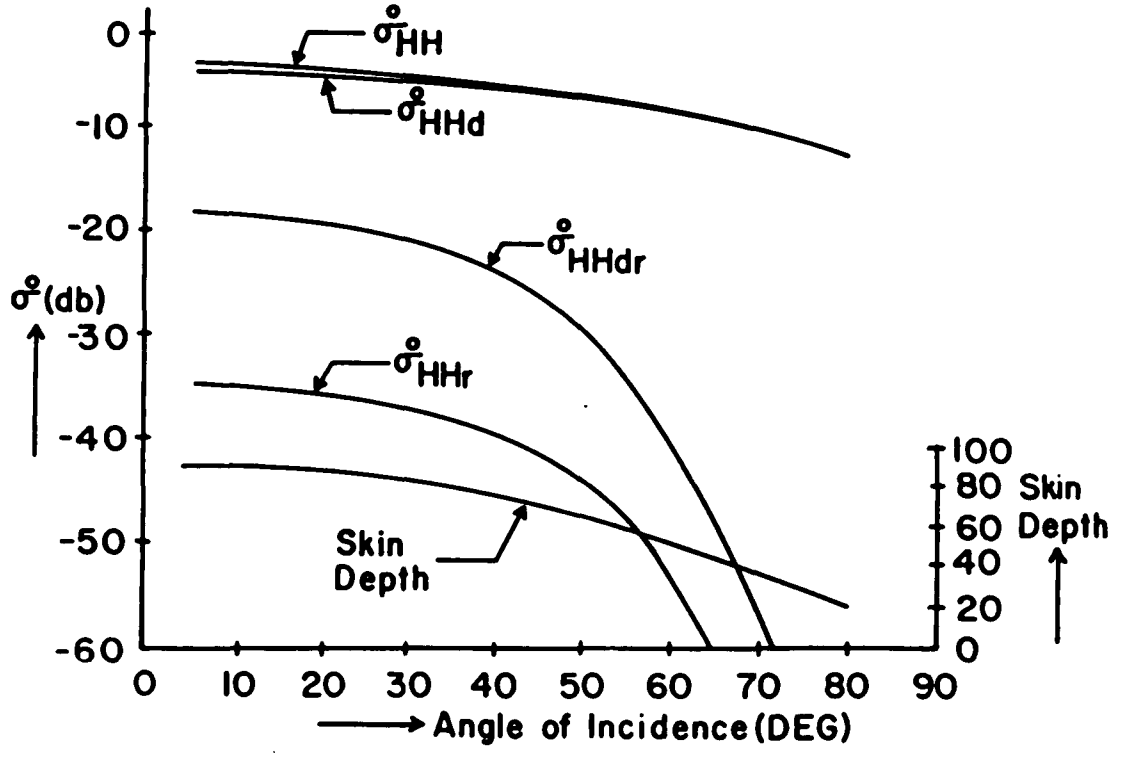

Fig. 6.2 Horizontal Copolarized Backscattering Cross Section vs. Angle of Incidence with d=100m, $\Delta\theta_{if}$=10°, ρ=500, f=400MHz, ε_r=30.8+i.0.62, ε_a=12+i3, a=7.5cm, and h=0.5mm.

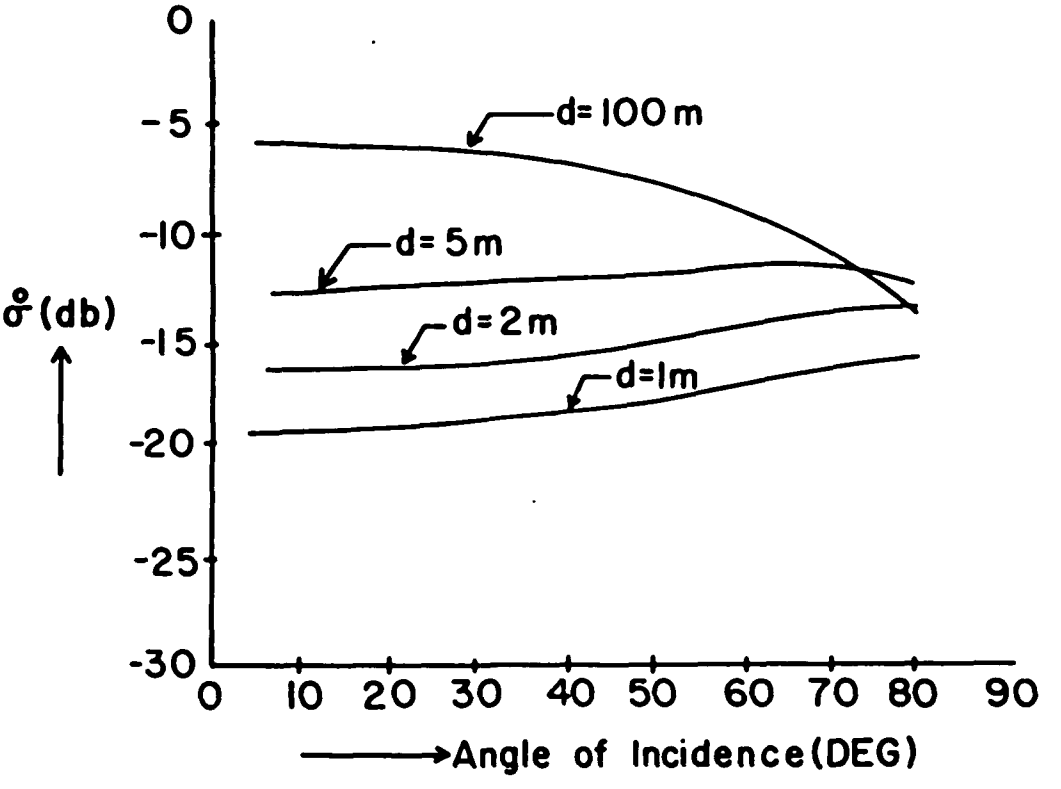

Fig. 6.3 Horizontal Copolarized Backscattering Cross Section with $\Delta\theta_i=10°$, $\rho=500$, f=400MHz, $\epsilon_r=30.8+i0.62$, $\epsilon_g=12+i3$, a=7.5cm and h=0.5mm.

ing curves make from a layer that is small compared to the skin depth (for d=1m) to a layer that is large compared to the skin depth (for d=100) is shown in the figure. The smaller values of 'd' correspond to the regime where Born approximation is valid, while the large values of 'd' agree with the half space results derived by Lang[27].

6.1.2 EFFECTS OF GROUND MOISTURE ON BACKSCATTERING COEFFICIENTS

To see the effects of moisture in the underlying ground, the following two different dielectric constants have been selected,

$$\epsilon_g = 12.0 + i3.0 \qquad \text{for dry ground}$$

and

$$\epsilon_g = 80.0 + i1.5 \qquad \text{for wet ground}$$

Fig.6.4 shows total backscattering coefficient σ^{o}_{hh} plotted for the above two different ground conditions and for two different layer thicknesses. For the case when d=1m, it is seen that there is a large difference in the backscattering coefficients for different ground moistures because the ground reflected terms are dominant. But when the layer thickness d=100m, the ground reflected terms are very small and their effect is masked when compared to the total backscattering coefficients. Therefore the ground condition becomes unimportant.

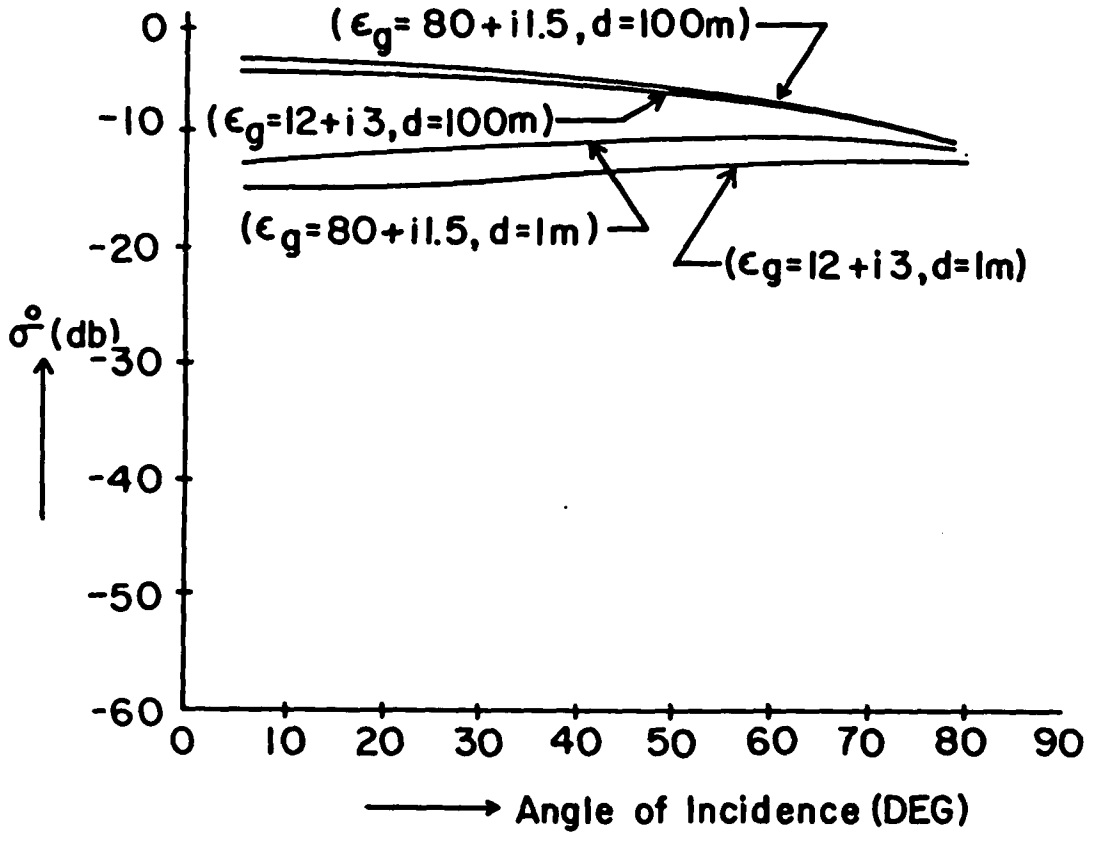

Fig. 64 Comparison of Horizontal Copolarized Backscattering Cross Sections for Different Ground Wetnesses and Different Vegetation Depths. $\Delta\theta_{1/2}$=10°, ρ=500, f=400MHz, ϵ_r=30.8+i0.62, a=7.5cm and h=0.5mm.

6.1.3 BACKSCATTERING COEFFICIENTS WITH PARALLEL DISTRIBUTION OF LEAVES

Fig. 6.5 shows the total backscattering coefficients σ^{o}_{hh}, σ^{o}_{vv} and σ^{o}_{vh} plotted for a parallel distribution of leaves. In this case, since the leaves are parallel to the horizontal polarization at all angles of incidence, backscattering coefficient σ^{o}_{hh} does not show any dependence on incidence angle.

6.1.4 BACKSCATTERING COEFFICIENTS WITH PERPENDICULAR DISTRIBUTION OF LEAVES

Fig. 6.6 shows the total backscattering coefficients σ^{o}_{hh}, σ^{o}_{vv} and σ^{o}_{vh} plotted for a perpendicular distribution of leaves. At small angles of incidence, σ^{o}_{vv} and σ^{o}_{hh} are equal, but as the angle of incidence increases, σ^{o}_{vv} decreases because the vertically polarized wave is becoming parallel to the leaves and thus getting more absorbed. On the other hand, σ^{o}_{hh} has a flat response because a changing angle of incidence does not affect the polarization orientation with respect to the leaves.

The backscattering cross section is higher in the parallel distribution case compared to the perpendicular distribution at small angles of incidence. Comparing σ^{o}_{vh} in Fig. 6.5 and Fig. 6.6, it can be concluded that the vertically inclined leaves give rise to more depolarization as compared to the horizontally inclined leaves.

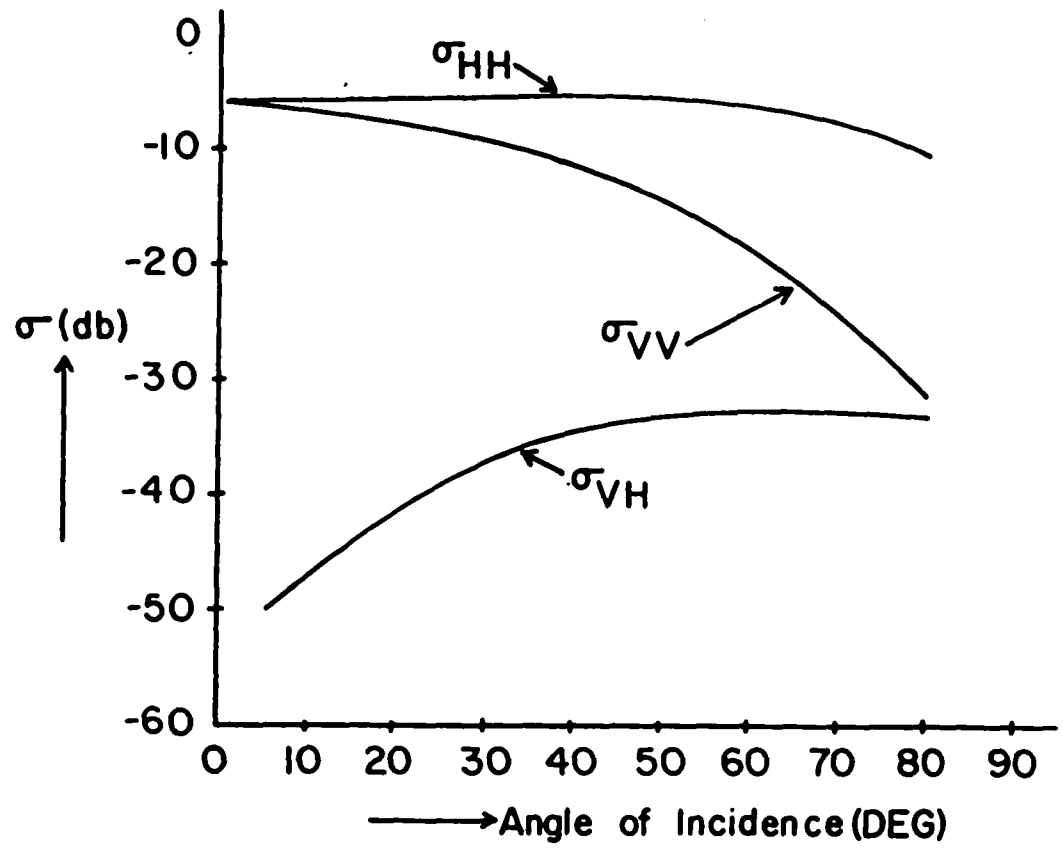

Fig. 6.5 Backscattering Coefficients vs. Angle of Incidence with d=10m, $\Delta\theta_i$=10°, ρ=500, f=400MHz, ϵ_r=30.8+i0.62, ϵ_g=12+i3, a=7.5 cm and h=0.5mm.

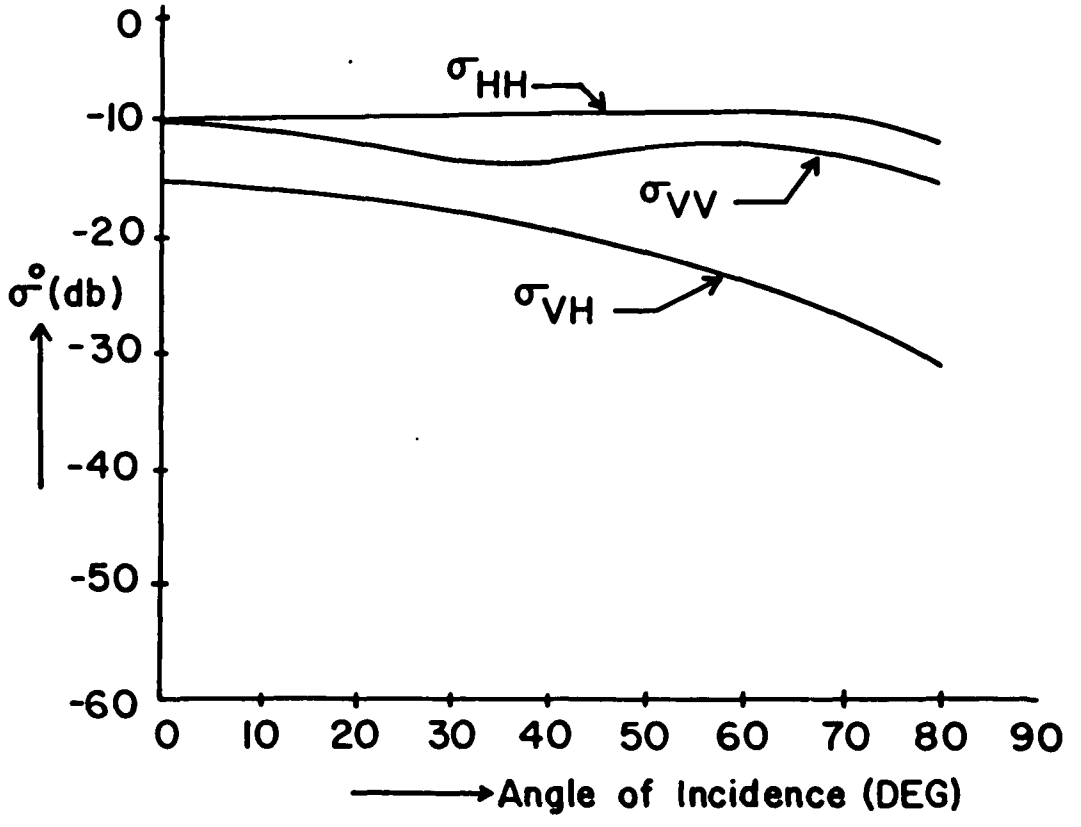

Fig. 6.6 Backscattering Coefficients vs. Angle of Incidence with d=10m, $\Delta\theta_{\perp}$=10°, ρ=500, f=400MHz, ϵ_r=30.8+i0.62, ϵ_g=12+i3, a=7.5cm and h=0.5mm.

6.2 MULTIPLE SCATTERING

A numerical method has been used to compute the backscattering coefficients as given in eqs.(5.38)-(5.41). Only zero-order equations have been solved, resulting in single scattering only. To determine the effect of multiple scattering, the zero-order result has to be used to solve the first-order equations in an iterative approach. Fig. 6.7 compares the results of the discrete method and the RTT method for single scattering. There is no significant difference in the backscattering coefficients. The copolarized coefficients are slightly less for RTT method than for the discrete method, but the cross polarized coefficient is greater for the RTT method above an incidence angle of about 20 degrees.

6.3 COMPARISON WITH OTHER PUBLISHED RESULTS

Similar results as shown in Fig. 6.5 and Fig. 6.6 have been observed by Tsang et al[43]. They have derived the backscattering cross sections using the vector radiative transport equations. In their backscattering equations results, only incoherent terms have been included. But in section 3.1, σ^{o}_{pqdr} as given in eqs.(3.9),(3.13) and (3.16) also include the coherent terms, where $p,q \in (h,v)$. According to the computations, the coherent effects are as important as the incoherent effects.This could be one of the reasons why backscattering cross sections in the present case are higher than Tsang et. al[43].

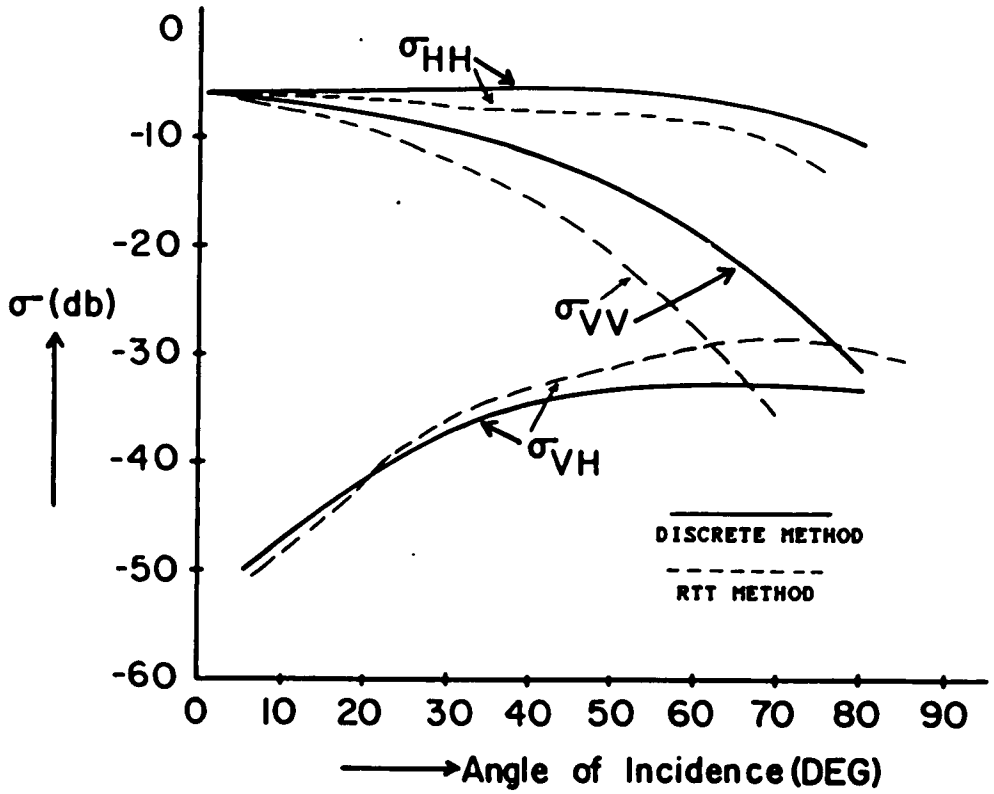

Fig 6.7 Backscattering coefficients vs. Angle of incidence with d=10m, $\Delta\theta_{\frac{1}{2}}$ = 10°, ρ=500, f=400 MHz, ϵ_r=30.8+i0.62, ϵ_g=12+i3.0, a=7.5 cm, and h=0.5 mm.

6.4 CONCLUSIONS AND COMPARISON WITH EXPERIMENTAL DATA

A comparison with the experimental data is shown in Fig. 6.8. Backscattering data from Soybeans at 1.8 Ghz by Oliver and Peake[32] has been used. The data were taken when the Soybeans were 30 to 36 inches high. The parameters in the model have been adjusted to give a reasonable agreement between experimental data and the theory as shown in Fig. 6.8. Since Rayleigh scatterers are being used to represent leaves at frequencies somewhat higher than the Rayleigh region, the model does not follow the data as closely for large angles of incidence.

These models work reasonably well when the wavelength is very large compared to the scatterers. This limits their use to frequencies around 1 GHz. An advantage of using the lower frequencies is that the electromagnetic wave will penetrate the vegetation more deeply, resulting in information about the lower vegetation layers and the ground underneath this vegetation.

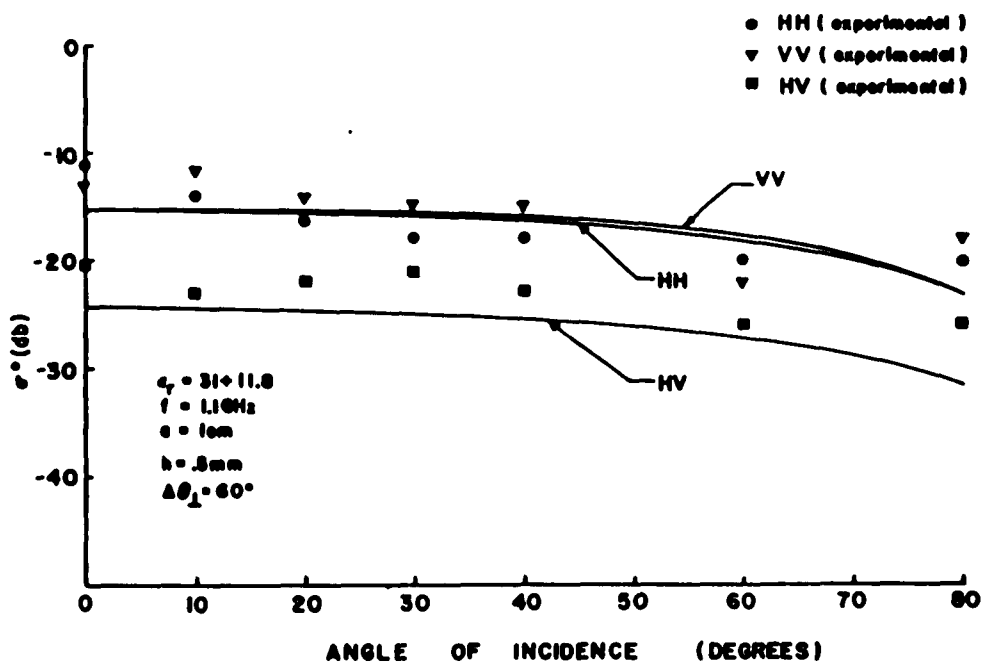

Fig. 6.8 Copolarized Backscattering coefficients vs. angle of incidence for $\Delta\theta_\perp = 60^\circ$, $\beta = 4000$, $f = 1.8$ GHz, $\epsilon_r = 35.8 \div 13.54$, $\epsilon_g = 1.2 \div 10.3$, $a = 2.25$ cm, $h = 0.5$ mm, and $d = 1$ m.

APPENDIX - A

DERIVATION OF GREEN'S FUNCTION

To compute the backscattering coefficients we have to evaluate the integral of $\bar{\bar{S}}(\bar{k}_t,q)$. To evaluate this, we will need the transformed Green's function in the equivalent medium. The procedure followed in this case will be similar to the one used to calculate mean field. The governing equation for Green's function as given by Lang[27] is,

$$[\nabla x(\nabla x\bar{\bar{I}})-k_o^2\bar{\bar{\epsilon}}_e(z)].\bar{\bar{G}}(\bar{x},\bar{x}') = \bar{\bar{I}}\delta(\bar{x}-\bar{x}') \qquad (A1)$$

Since the Green's function is homogeneous in the transverse direction, by taking the transverse Fourier transform of both sides of the above equation and simplifying, we obtain

$$[k_{x_o}^2(\bar{y}^o\bar{y}^o+\bar{z}^o\bar{z}^o) + ik_{x_o}\frac{\partial}{\partial z}(\bar{z}^o\bar{x}^o+\bar{x}^o\bar{z}^o) - \frac{\partial^2}{\partial z^2}(\bar{x}^o\bar{x}^o+\bar{y}^o\bar{y}^o)$$

$$-k_o^2\bar{\bar{\epsilon}}_e(z)].\bar{\bar{G}}(\bar{k}_t,z,z') = \bar{\bar{I}}\delta(z-z_o) \qquad (A2)$$

where $\bar{k}_t = k_{x_o}\bar{x}^o$ and $\bar{\bar{\epsilon}}_e(z)$ is given by eq.(2.3).

Since eq.(A2) is a dyadic equation, it is equivalent to nine scalar equations. Four of these equations involve only the dependent variables G_{xy}, G_{zy}, G_{yx} and G_{yz}. Since these equations have no forcing function and satisfy homogeneous boundary conditions (radiation condition), their solution

must be

$$G_{xy} = G_{zy} = G_{yx} = G_{yz} = 0 \quad , \qquad |z|<\infty \tag{A3}$$

The remaining five equations are

$$\left(\frac{\partial^2}{\partial z^2} + k_o^2 \epsilon_{yy}(z) - k_{x_o}^2\right) G_{yy} = -\delta(z-z_o) \tag{A4}$$

$$\left(\frac{\partial^2}{\partial z^2} + k_o^2 \epsilon_{xx}(z)\right) G_{xx} - ik_{x_o} \frac{\partial}{\partial z} G_{zx} = -\delta(z-z_o) \tag{A5}$$

$$-ik_{x_o} \frac{\partial}{\partial z} G_{xx} + \left(k_o^2 \epsilon_{zz}(z) - k_{x_o}^2\right) G_{zx} = 0 \tag{A6}$$

$$-ik_{x_o} \frac{\partial}{\partial z} G_{xz} + \left(k_o^2 \epsilon_{zz}(z) - k_{x_o}^2\right) G_{zz} = -\delta(z-z_o) \tag{A7}$$

$$\left(\frac{\partial^2}{\partial z^2} + k_o^2 \epsilon_{xx}(z)\right) G_{xz} - ik_{x_o} \frac{\partial}{\partial z} G_{zz} = 0 \tag{A8}$$

where $G_{ij} = G_{ij}(\bar{k}_t, z, z_o)$.

Since G_{yy} given in eq.(A4) is the simplest equation, so let us examine it first. We will solve this equation approximately by utilizing the two variable method. The boundary conditions to be used are that $\bar{G}_{yy}(k_t, z, z_o)$ and $\partial \bar{G}_{yy}(k_t, z, z_o)/\partial z$ must be continuous at z=0 and z=-d. In addition, G_{yy} must be continuous at the source and satisfy the jump condition.

Proceeding in the same manner as for the mean wave case, and assuming that the unit source is inside the slab, i.e. $0>z_o>-d$, we find that solution for $\bar{G}_{yy}(k_t, z, z_o)$ has the following form,

$$G_{yy}(\bar{k}_t,z,z_o) = \begin{cases} T_{oy}e^{ik_o(\cos\theta_o z+\sin\theta_o x)} & , z>0 \quad (A9) \\ T_{oy}e^{ik_z^{(h)}z}\, e^{ik_o\sin\theta_o x} & , 0>z>z_o \quad (A10) \\ T_{oy}e^{-ik_z^{(h)}z}\, e^{ik_o\sin\theta_o x} & , z>z_o>-d \quad (A11) \\ T_{1y}e^{-ik_{z_g}z}\, e^{ik_o\sin\theta_o x} & , z<-d \quad (A12) \end{cases}$$

where $$T_{oy} = -\frac{1}{2ik_{z_o}}(1+\Gamma_o^{(h)}e^{-2ik_z^{(h)}z_o})e^{ik_z^{(h)}z_o} \quad (A13)$$

$$T_{1y} = -\frac{1}{2ik_{z_o}}\left(\frac{k_{z_g}}{k_{z_o}+k_{z_g}}\right)e^{-ik_{z_g}d}\, e^{ik_z^{(h)}(d-z_o)} \quad (A14)$$

and where $\Gamma_o^{(h)}$ and $k_z^{(h)}$ are defined in eqs.(2.47) and (2.49) respectively, and $k_{z_g} = \sqrt{k_o^2\epsilon_g - k_{x_o}^2}$.

Following a similar procedure, we can find solutions for G_{xx}, G_{zx}, G_{xz} and G_{zz} from eqs.(A5)-(A8). We are interested in the solution for the Green's function only in the region $0>z>z_o$. Thus by collecting all the solutions in this region, we find

$$\begin{aligned} \bar{G}(\bar{k}_t,z,z_o) = [&T_{ox}e^{ik_z^{(v)}z}\bar{x}_o\bar{x}_o + T_{oy}e^{ik_z^{(h)}z}\bar{y}_o\bar{y}_o \\ &-\tan\theta_o T_{ox}e^{ik_z^{(v)}z}\bar{z}_o\bar{x}_o + T_{oz}e^{ik_z^{(v)}z}\bar{x}_o\bar{z}_o \\ &-\tan\theta_o T_{oz}e^{ik_z^{(v)}z}\bar{z}_o\bar{z}_o\,].e^{ik_o\sin\theta_o x} \end{aligned}$$

$$0>z>z_o \quad (A15)$$

where

$$T_{ox} = -\frac{\cos^2\theta_o}{2ik_{z_o}} (1-r_o^{(v)} e^{-2ik_z^{(v)} z_o}) e^{ik_z^{(v)} z_o} \qquad (A16)$$

$$T_{oz} = -\frac{\sin\theta_o \cos\theta_o}{2ik_{z_o}} (1+r_o^{(v)} e^{-2ik_z^{(v)} z_o}) e^{ik_z^{(v)} z_o} \qquad (A17)$$

and T_{oy} is as given by eq.(A13).

Rearranging eq.(A15) and writing results in terms of $\bar{h}^o, \bar{v}_-^o$ and $\bar{v}_+^o$ we can write

$$\bar{G}(\bar{k}_t, z, z_o) = \frac{1}{2ik_{z_o}} [(e^{ik_z^{(h)} z_o} + r_o^{(h)} e^{-ik_z^{(h)} z_o}) e^{ik_z^{(h)} z} \bar{h}^o \bar{h}^o + (e^{ik_z^{(v)} z_o} \bar{v}_-^o \bar{v}_-^o + r_o^{(v)} e^{-ik_z^{(v)} z_o} \bar{v}_-^o \bar{v}_+^o) . e^{ik_z^{(v)} z}]$$

$$0 > z > z_o \qquad (A18)$$

where $\bar{h}^o$ and $\bar{v}_\pm^o$ are given by eqs.(2.24) and (2.25) respectively.

APPENDIX - B

PHASE MATRIX 'P' AND EXTINCTION MATRIX 'K' EVALUATION IN A THIN DISC

In order to determine the 16 elements of the phase matrix, we have to first calculate the fields scattered by a plane wave of arbitrary polarization incident on an arbitrarily oriented disk. The orientation of the disk is described by the Eulerian angles $(\Theta,\emptyset,\tau)$ as shown in Fig. B.1. In terms of these angles, normal to the disk $\bar{n}^o$ is,

$$\bar{n}^o = \text{Sin}\Theta(\text{Sin}\emptyset\ \bar{X}^o - \text{Cos}\emptyset\ \bar{Y}^o) + \text{Cos}\Theta\ \bar{Z}^o \qquad (B.1)$$

Fig. B.2 shows the problem geometry, where an incident wave $\bar{i}^o(\Theta_i,\emptyset_i)$ has been scattered by the disk into a scattered wave $\bar{o}^o(\Theta_i,\emptyset_i)$. We will assume that the fields inside the disk are the same as those that would exist in a dielectric slab of the same thickness and orientation as the disk. This approximation is good when the edge effects are small, such as in the case when the edge cross section of the disk is large compared to the wavelength and large compared to the thickness of the disk.

B.1 SCATTERED FIELD

A plane wave of unit amplitude and polarization $\bar{q}$ is incident upon the disk, such that

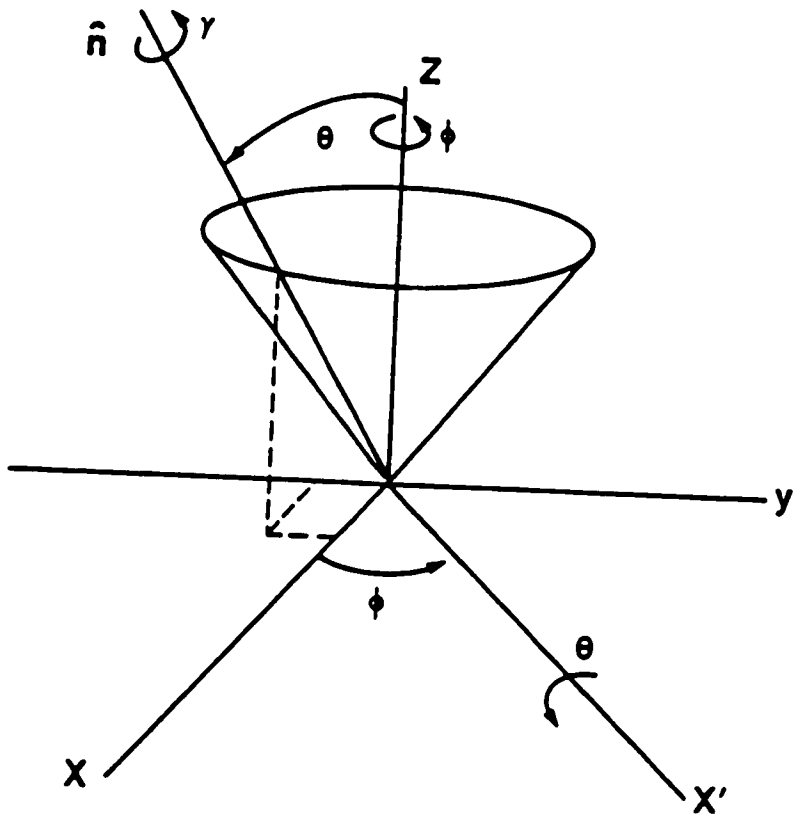

Fig. B.1 Eulerian angles $(\Theta,\emptyset,\tau)$ which describe the disk orientation

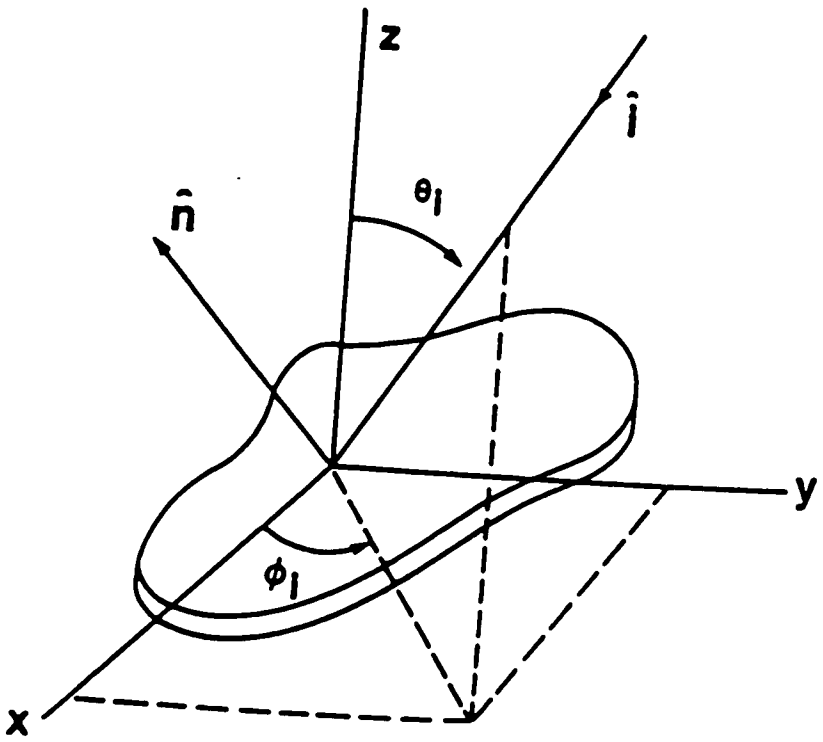

Fig. B.2 Problem Geometry

$$\bar{E}_o(x,q) = q\, e^{-o\ i\bar{k}.\bar{x}} \qquad q\epsilon\{h,v\} \qquad (B.2)$$

where $\bar{k}$ is the assumed direction of propagation.

The disk is assumed to have a cross sectional shape 'S', a thickness 'T' and relative dielectric permittivity ϵ_r. It will be assumed that the permittivity ϵ_r is constant across the disk.

The solution for the scattered fields can be obtained in terms of the fields inside the disk by solving the radiation from induced polarization and conduction currents following standard procedures as described by Ito and Adachi[17] and Jones[18]. The scattered field will be given by,

$$\bar{E}_s(\bar{x},q) = k_o^2 \int_{disk} (\epsilon_r - 1).\bar{\bar{G}}(\frac{\bar{x}}{\bar{x}'}).\bar{E}(\bar{x}',q)d\bar{x}' \qquad (B.3)$$

where the integration is over the volume of the disk and $\bar{\bar{G}}(\frac{\bar{x}}{\bar{x}'})$ is the free space dyadic Green's function given by Keller[22] as,

$$\bar{\bar{G}}(\frac{\bar{x}}{\bar{x}'}) = [\bar{\bar{I}} + \frac{1}{k_o^2}\bar{\nabla}\bar{\nabla}]\frac{e^{jk_oR}}{4\pi R} \qquad (B.4)$$

where $R = \bar{x}-\bar{x}'$ and $\bar{\bar{I}}$ is the unit dyadic. Using an asymptotic expression that the fields inside the disk are the same as those that would exist in a dielectric slab of the same thickness and orientation as the disk, from Levine et al[31], we get

$$\bar{E}_s(\bar{x}) = \bar{\bar{f}}(\bar{o},\bar{i})\,\frac{e^{ik_o R}}{R} \qquad (B.5)$$

where $\bar{\bar{f}}(o,i)$ is the dyadic scattering amplitude.

B.2 VECTOR SCATTERING AMPLITUDE

The vector scattering amplitudes are related to the dyadic scattering amplitude as,

$$\bar{\bar{f}}(\bar{o},\bar{i}) = \bar{\bar{f}}(\bar{o},\bar{i};h)\bar{h}^o + \bar{\bar{f}}(\bar{o},\bar{i};v)\bar{v}^o \qquad (B.6)$$

and in thin disc case,

$$\bar{f}(\bar{o},\bar{i};q) = \frac{k_o^2 x T}{4\pi}(\bar{\bar{I}}-\bar{o}.\bar{o})\left[\bar{q}^o - \frac{x}{x+1}(\bar{n}^o.\bar{q}^o)\bar{n}^o\right]S(\bar{\tau}_t) \qquad (B.7)$$

where $S(\bar{\tau}_t) = \frac{a}{\tau} J_1(2\pi\tau a)$ (B.8)

$$x = \epsilon_r - 1 \qquad (B.9)$$

and $\tau = \frac{k_o}{2\pi}\sqrt{\alpha^2 + \beta^2}$ (B.10)

where,

$$\alpha = \mathrm{Cos}\theta\left[\mathrm{Sin}\theta_i \mathrm{Sin}(\phi-\phi_i) + \mathrm{Sin}\theta_s \mathrm{Sin}(\phi-\phi_s)\right] - \mathrm{Sin}\theta\left[\mathrm{Cos}\theta_i + \mathrm{Cos}\theta_s\right] \qquad (B.11A)$$

and $\beta = \mathrm{Sin}\theta_i \mathrm{Cos}(\phi-\phi_i) + \mathrm{Sin}\theta_s \mathrm{Cos}(\phi-\phi_s)$ (B.11B)

B.3 DYADIC SCATTERING AMPLITUDES

From eq.(B.6), the Dyadic scattering amplitude is given as,

$$f_{qq}(\bar{o}^o,\bar{i}^o)=\bar{q}^o.\bar{\bar{f}}_{qq}(\bar{o},\bar{i}).\bar{q}^o=\bar{q}^o.[\bar{f}(\bar{o}^o,\bar{i}^o;h)\bar{h}^o+\bar{f}(\bar{o}^o,\bar{i}^o;v)\bar{v}^o].\bar{q}^o \tag{B.12}$$

B.3.1 HH CASE

In the case when the incident and scattered waves are horizontally polarized,

$$f_{hh}(\bar{o},\bar{i}) = \frac{k_o^2 x T}{4\pi}[\bar{h}_s^o.\bar{h}_i^o - \frac{x}{x+1}(\bar{n}^o.\bar{h}_i^o)(\bar{n}^o.\bar{h}_s^o)]S(\bar{\tau}_t)$$

or

$$f_{hh}(\bar{o},\bar{i})=\frac{k_o^2 x T}{4\pi}[-\mathrm{Cos}(\phi_s-\phi_i)+\frac{x}{x+1}\mathrm{Sin}\theta\mathrm{Cos}(\phi-\phi_i)\mathrm{Sin}\theta\mathrm{Cos}(\phi-\phi_s)]S(\bar{\tau}_t) \tag{B.13}$$

Therefore,

$$\langle |f_{hh}(\bar{o},\bar{i})|^2\rangle = \frac{k_o^4 |x|^2 T^2}{(4\pi)^2}\int_o^{\pi} d\theta p(\theta)\int_o^{2\pi}\frac{1}{2\pi}\,d\phi\;|-\mathrm{Cos}(\phi_s-\phi_i)$$

$$+\frac{x}{x+1}\mathrm{Sin}^2\theta\mathrm{Cos}(\phi-\phi_i)\mathrm{Cos}(\phi-\phi_s)|^2|S(\bar{\tau}_t)|^2 \tag{B.14}$$

Using a Fourier series expansion and equating, we get

$$\langle |f_{hhm}(\bar{\theta},\bar{\theta}')|^2 \rangle = \frac{k_o^4 |x|^2 T^2}{(4\pi)^2} \frac{1}{(2\pi)^2} \int_0^{2\pi} d\bar{\phi}_d \int_0^{\pi} d\bar{\theta} p(\bar{\theta}) \int_0^{2\pi} d\bar{\phi} \; |1-\cos\phi_d$$

$$+ \frac{x}{x+1} \sin^2\bar{\theta} \cos\bar{\phi} \cos(\bar{\phi}-\bar{\phi}_d)|^2 \; e^{-im\phi_d} . (\pi a^2)^2 \qquad (B.15)$$

where $$\phi_d = \phi_s - \phi_i \qquad (B.16)$$

Integrating and simplifying, we get

$$\langle |f_{hhm}(\bar{\theta},\bar{\theta}')|^2 \rangle = \begin{cases} C_a \int_0^{\pi} d\bar{\theta} p(\bar{\theta}) \left[2 + \left|\frac{x}{x+1}\right|^2 \sin^4\bar{\theta} - 2\mathrm{Re}\left(\frac{x}{x+1}\right)\sin^2\bar{\theta}\right] & \text{for } m = 0 \\ C_a \int_0^{\pi} d\bar{\theta} p(\bar{\theta}) \left[1 + \left|\frac{x}{x+1}\right|^2 . \frac{1}{4}\sin^4\bar{\theta} - \mathrm{Re}\left(\frac{x}{x+1}\right)\sin^2\bar{\theta}\right] & \text{for } m = \pm 2 \end{cases}$$

(B.17)

where $$C_a = \frac{K_o^4 |x|^2 T^2 a^4}{64} \qquad (B.17a)$$

B.3.2 VV CASE

Similarly, when incident and scattered waves are vertically polarized, we have

$$\langle |f_{vvm}(\bar{\theta},\bar{\theta}')|^2 \rangle = \frac{k_o^4 |x|^2 T^2}{64\pi^4} \int_0^{2\pi} d\bar{\phi}_d \int_0^{\pi} d\bar{\theta} p(\bar{\theta}) \int_0^{2\pi} d\bar{\phi} \, |\{\cos\theta\cos\theta'\cos\phi_d$$

$$+\sin\theta\sin\theta'\} - \frac{x}{x+1} \{-\sin\bar{\theta}\cos\theta'\sin\bar{\phi} + \cos\bar{\theta}\sin\theta'\}$$

$$. \{-\sin\bar{\theta}\cos\theta\sin(\bar{\phi}-\bar{\phi}_d) + \cos\bar{\theta}\sin\theta\}|^2 . (\pi a^2)^2 . e^{-im\phi_d}$$

(B.18)

Therefore integrating and simplifying, we get

$$\langle |f_{vvm}(\theta,\theta')|^2 \rangle = \begin{cases} C_a \int_0^{\pi} d\bar{\theta} p(\bar{\theta}) [-2Re(\frac{x}{x+1}) Cos^2\theta Cos^2\theta' Sin^2\bar{\theta}] \\ \qquad\qquad\qquad\qquad\qquad\qquad \text{for } m = 0 \\ C_a \int_0^{\pi} d\bar{\theta} p(\bar{\theta}) [4Cos\theta Cos\theta' Sin\theta Sin\theta' \\ \quad + \left|\frac{x}{x+1}\right|^2 (Sin^4\bar{\theta} Cos^2\theta' Cos^2\theta \\ \quad + Sin^2\theta Cos\theta' Cos^2\theta Sin\theta' Cos\theta Sin\theta) \\ \quad -2Re(\frac{x}{x+1}) (Sin^2\theta Cos\theta' Cos\theta Sin\theta Sin\theta' \\ \quad + 2Cos\theta Cos\theta' Cos^2\bar{\theta} Sin\theta Sin\theta')] \\ \qquad\qquad\qquad\qquad\qquad\qquad \text{for } m = \pm 1 \\ C_a \int_0^{\pi} d\bar{\theta} p(\bar{\theta}) [Cos^2\theta Cos^2\theta' \\ \quad + \left|\frac{x}{x+1}\right|^2 Sin^4\bar{\theta} Cos^2\theta' Cos^2\theta . \frac{1}{4} \\ \quad -2Re(\frac{x}{x+1}) . Cos^2\theta Cos^2\theta' Sin^2\bar{\theta}] \\ \qquad\qquad\qquad\qquad\qquad\qquad \text{for } m = \pm 2 \end{cases} \qquad (B.19)$$

where C_a is as given in eq. (B.17a).

B.3.3 HV and VH CASES

When one of the incident or scattered waves is vertically

polarized, we have

$$\langle |f_{hvm}(\bar{\theta},\bar{\theta}')|^2 \rangle = \langle |f_{vhm}(\bar{\theta},\bar{\theta}')|^2 \rangle = \frac{k_o^4 |x|^2 T^2 a^4}{64\pi^4} \int_0^{2\pi} d\bar{\phi}_d \int_0^{\pi} d\bar{\theta} p(\bar{\theta}) \int_0^{2\pi} d\bar{\phi}$$

$$|-\cos\theta' \sin\phi_d - \frac{x}{x+1} \{-\sin\bar{\theta} \cos\theta' \sin\bar{\phi} + \cos\bar{\theta} \sin\theta'\}$$

$$. \{\sin\bar{\theta} \cos(\bar{\phi}-\phi_d)\}|^2 (\pi a^2)^2 \, e^{-im\phi_d}$$

(B.20)

Performing the integration and simplifying, we get

$$\langle |f_{hvm}(\theta,\theta')|^2 \rangle = \begin{cases} C_a \cos^2\theta' \int_0^{\pi} d\bar{\theta} p(\bar{\theta}) [-\left|\frac{x}{x+1}\right|^2 \sin^4\bar{\theta} \\ \quad + 2\mathrm{Re}\left(\frac{x}{x+1}\right) \sin\bar{\theta}] \\ \qquad \text{for } m = 0 \\ -m\, C_a \cos^2\theta' \int_0^{\pi} d\bar{\theta} p(\bar{\theta}) \\ \qquad \text{for } m = \pm 1 \\ C_a [-\left|\frac{x}{x+1}\right|^2 \frac{1}{4} \cos^2\theta' \int_0^{\pi} d\bar{\theta} p(\bar{\theta}) \sin^4\bar{\theta} \\ -\mathrm{Re}\left(\frac{x}{x+1}\right) \cos^2\theta' \int_0^{\pi} d\bar{\theta} p(\bar{\theta}) \sin\bar{\theta}] \\ \qquad \text{for } m = \pm 2 \end{cases}$$

(B.21A)

where C_a is as given in eq.(B.17).

and

$$\langle |f_{vhm}(\theta,\theta')|^2 \rangle = \langle |f_{hvm}(\theta,\theta')|^2 \rangle \qquad \text{(B.21B)}$$

Similarly,

$$\langle [f_{vv}(\theta,\theta') f^*_{vh}(\theta,\theta')]_m \rangle = \begin{cases} \mp i C_a \, \mathrm{Sin}\theta \mathrm{Sin}\theta' \int_0^{\pi} d\bar{\theta} p(\bar{\theta}) [2\mathrm{Cos}\theta' \\ \quad + (\frac{x}{x+1}) 2\mathrm{Cos}^2\theta \mathrm{Cos}\theta' - (\frac{x}{x+1})^* \mathrm{Sin}^2\bar{\theta}\mathrm{Cos}\theta \\ \quad + \left|\frac{x}{x+1}\right|^2 \mathrm{Sin}^2\bar{\theta}\mathrm{Cos}^2\bar{\theta}\mathrm{Cos}\theta'] \\ \qquad\qquad \text{for } m = \pm 1 \\ C_a \, \mathrm{Cos}^2\theta \mathrm{Cos}\theta' \int_0^{\pi} d\bar{\theta} p(\bar{\theta}) [1 - \mathrm{Re}(\frac{x}{x+1}) \mathrm{Sin}^2\bar{\theta} \\ \quad + \frac{1}{4} \left|\frac{x}{x+1}\right|^2 \mathrm{Sin}^4\bar{\theta}] \\ \qquad\qquad \text{for } m = \pm 2 \end{cases} \qquad \text{(B.22)}$$

$$\langle [f_{hv}(\theta,\theta') f^*_{hh}(\theta,\theta')]_m \rangle = i C_a 2\mathrm{Cos}\theta' \int_0^{\pi} d\bar{\theta} p(\bar{\theta}) [1 + \mathrm{Im}(\frac{x}{x+1}) \mathrm{Sin}^2\bar{\theta} + \frac{1}{4} \left|\frac{x}{x+1}\right|^2 \mathrm{Sin}^4\bar{\theta}] \qquad \text{(B.23)}$$

and

$$
\begin{aligned}
&\langle [f_{vv}(\theta,\theta')f_{hh}(\theta,\theta') \pm f_{vh}(\theta,\theta')f_{hv}(\theta,\theta')] \rangle = \\
&\quad C_a \mathrm{Cos}\theta\mathrm{Cos}\theta' \int_0^{\pi} d\bar{\theta}\, p(\bar{\theta}) \Big[(-2 \pm 2) \\
&\qquad + 2\mathrm{Re}\left(\frac{x}{x+1}\right)(\mathrm{Sin}^2\bar{\theta} \mp \mathrm{Sin}^2\bar{\theta}) + \frac{3}{4}\left|\frac{x}{x+1}\right|^2 \mathrm{Sin}^4\bar{\theta} \Big] \\
&\qquad\qquad \text{for } m = 0 \\
&\quad C_a \mathrm{Sin}\theta\mathrm{Sin}\theta' \int_0^{\pi} d\bar{\theta}\, p(\bar{\theta}) \Big[-2 + \frac{x}{x+1}(2\mathrm{Cos}^2\bar{\theta}) \\
&\qquad + \left(\frac{x}{x+1}\right)\mathrm{Sin}^2\bar{\theta} - \left|\frac{x}{x+1}\right|^2 \mathrm{Cos}^2\bar{\theta}\mathrm{Sin}^2\bar{\theta} \Big] \\
&\qquad\qquad \text{for } m = \pm 1 \\
&\quad C_a\, \mathrm{Cos}\theta\mathrm{Cos}\theta' \int_0^{\pi} d\bar{\theta}\, p(\bar{\theta}) \Big[(-1 \mp 1) \\
&\qquad + \mathrm{Re}\left(\frac{x}{x+1}\right)(\mathrm{Sin}^2\bar{\theta} \pm \mathrm{Sin}^2\bar{\theta}) \\
&\qquad - \frac{1}{4}\left|\frac{x}{x+1}\right|^2 (\mathrm{Sin}^4\bar{\theta} \mp \frac{3}{2}\mathrm{Sin}^4\bar{\theta}) \Big] \\
&\qquad\qquad \text{for } m = \pm 2
\end{aligned}
\tag{B.24}
$$

where C_a is as given in eq. (B.17a).

B.4 ZERO ORDER PHASE MATRIX $\bar{\bar{P}}_o(\theta,\theta')$

Elements of the phase matrix can be expanded into a Fourier series as follows,

$$
\bar{\bar{P}}(\theta,\theta',\phi-\phi') = \sum_{m=-\infty}^{\infty} \bar{\bar{P}}_m(\theta,\theta') e^{im(\phi-\phi')} \tag{B.25}
$$

and comparing elements of the same order, we get

$$\bar{P}(\theta,\theta') = \begin{bmatrix} \langle |f_{vvo}(\theta,\theta')|^2 \rangle & \langle |f_{vho}(\theta,\theta')|^2 \rangle & \mathrm{Re}\langle f_{vvo}(\theta,\theta') f^*_{vho}(\theta,\theta') \rangle & -\mathrm{Im}\langle f_{vvo}(\theta,\theta') f^*_{vho}(\theta,\theta') \rangle \\ \langle |f_{hvo}(\theta,\theta')|^2 \rangle & \langle |f_{hho}(\theta,\theta')|^2 \rangle & \mathrm{Re}\langle f_{hvo}(\theta,\theta') f^*_{hho}(\theta,\theta') \rangle & -\mathrm{Im}\langle f_{hvo}(\theta,\theta') f^*_{hho}(\theta,\theta') \rangle \\ 2\mathrm{Re}\langle f_{vvo}(\theta,\theta') f^*_{hvo}(\theta,\theta') \rangle & 2\mathrm{Re}\langle f_{vho}(\theta,\theta') f^*_{hho}(\theta,\theta') \rangle & \mathrm{Re}\langle f_{vvo}(\theta,\theta') f^*_{hho}(\theta,\theta') + f_{vho}(\theta,\theta') f^*_{hvo}(\theta,\theta') \rangle & -\mathrm{Im}\langle f_{vvo}(\theta,\theta') f^*_{hho}(\theta,\theta') - f_{vho}(\theta,\theta') f^*_{hvo}(\theta,\theta') \rangle \\ 2\mathrm{Im}\langle f_{vvo}(\theta,\theta') f^*_{hvo}(\theta,\theta') \rangle & 2\mathrm{Im}\langle f_{vho}(\theta,\theta') f^*_{hho}(\theta,\theta') \rangle & \mathrm{Im}\langle f_{vvo}(\theta,\theta') f^*_{hho}(\theta,\theta') + f_{vho}(\theta,\theta') f^*_{hvo}(\theta,\theta') \rangle & \mathrm{Re}\langle f_{vvo}(\theta,\theta') f^*_{hho}(\theta,\theta') - f_{vho}(\theta,\theta') f^*_{hvo}(\theta,\theta') \rangle \end{bmatrix} \tag{B.26}$$

Substituting from section B.3 results, we get

$$\bar{P}(\theta,\theta') = \begin{bmatrix} \langle |f_{vvo}(\theta,\theta')|^2 \rangle & \langle |f_{vho}(\theta,\theta')|^2 \rangle & 0 & 0 \\ \langle |f_{hvo}(\theta,\theta')|^2 \rangle & \langle |f_{hho}(\theta,\theta')|^2 \rangle & 0 & 0 \\ 0 & 0 & \mathrm{Re}\langle f_{vv}(\theta,\theta') f^*_{hh}(\theta,\theta') - f_{vh}(\theta,\theta') f^*_{hv}(\theta,\theta') \rangle & 0 \\ 0 & 0 & 0 & \mathrm{Re}\langle f_{vv}(\theta,\theta') f^*_{hh}(\theta,\theta') - f_{vh}(\theta,\theta') f^*_{hv}(\theta,\theta') \rangle \end{bmatrix} \tag{B.27}$$

B.5 ZERO ORDER EXTINCTION MATRIX $\bar{R}_o(\theta)$

Since the extinction matrix represents absorption and scattering losses in the forward direction ($\theta=\theta'$), using results from section B.3 and B.4, we get

$$Re(f_{hvo}(\theta)) = Re(f_{vho}(\theta)) = 0$$

Therefore,

$$\bar{R}_o(\theta) = \begin{bmatrix} 2Re(M_{hho}) & 0 & 0 & 0 \\ 0 & 2Re(M_{vvo}) & 0 & 0 \\ 0 & 0 & Re(M_{hho}+M_{vvo}) & 0 \\ 0 & 0 & 0 & Re(M_{hho}+M_{vvo}) \end{bmatrix} \quad (B.28)$$

where $$M_{pqo} = i\frac{2\pi}{k}\langle f_{pqo}(\theta,\theta')_{\theta=\theta'}\rangle \qquad p,q \in \{h,v\} \quad (B.29)$$

and

$$\langle f_{hho}(\theta)\rangle = \frac{k_o^2 xT(\pi a^2)}{4\pi}\left[1-\frac{x}{2(x+1)}\int_0^{\pi} d\theta' p(\theta')\sin^2\theta'\right] \quad (B.30)$$

$$\langle f_{vvo}(\theta)\rangle = \frac{k_o^2 xT(\pi a^2)}{4\pi}\left[1-\frac{x}{2(x+1)}\{2\sin^2\theta + (\cos^2\theta-2\sin^2\theta)\int_0^{\pi} d\theta' p(\theta')\cos^2\theta'\}\right] \quad (B.31)$$

B.6 RECIPROCITY PROPERTY OF THE PHASE MATRIX

If the directions of the incident and scattered beams are interchanged, then it follows that Θ is to be replaced by Θ' and $\emptyset$ by $\emptyset+\pi$. The zero order phase matrix, as given by eq.(B.27), is independent of the $\emptyset$ variable, and from eq.(B.21B) it can be seen that 'h' and 'v' terms are interchangeable. Therefore we see that interchanging the incident and scattered beams results in a phase matrix which is the transpose of the original phase matrix,

$$P(\Theta',\Theta) = \text{tr } P(\Theta,\Theta') \qquad \text{(B.32)}$$

This shows that this phase matrix has the reciprocity property.

REFERENCES

1. Brown,W.P.Jr. IEEE Trans. Antenna Propagation. 1967, AP-15, 81-89.

2. Carlson,N.L. Tech. report, Electro Science Lab., Ohio State Univ. Columbus, OH. 1967, 1903-1905.

3. Chandrasekhar,S. "Radiative Transfer"; Dover Publications Inc.: New York, 1960

4. Cheung,R.L.; Ishimaru,A. Applied Optics 1982, Vol.21, No.20, 3792-3798.

5. Collin,R.E.; Zucker,F.J. "Antenna Theory", Part 1, McGraw Hill: New York, 1969, p41-43.

6. de Loor,G.P. J. Microwave Power, 1968, Vol.3, p67-73.

7. de Wolf,D. IEEE Trans. Antenna Propagation,1971, AP-19, p254-292.

8. Du, L.; Peake,W.H. Proc. IEEE 1969, Vol.57, No.6, p1227-1229.

9. Foldy,L. Phys. Rev. 1945, Vol.67, No.3, p107-119.

10. Fung,A.; Fung,H. IEEE Trans. Geosci. Electron. 1977, Vol.15, No.4, p189-195.

11. Fung,A.; Ulaby,F. IEEE Trans. Geosci. Electron.1978, Vol.16, No.4, p281-286.

12. Fung,A. IEEE Trans. Geosci. Electron.1979, Vol.17, NO.1, p1-6.

13. Fung,A.K.; CHEN,M.F. Radio Sci.1981, Vol.16, No.6, p1337-1347.

14. Hevnor,R. Tech. Report ETL-0105, U.S.Army Engineer Topogra. Lab.1976, Ft. Belvoir, VA.

15. Ishimaru,A. "Wave propagation and scattering in random media", Vol.1 and 2, Academic Press: New York, 1978

16. Ishimaru,A. JOSA, 1978, Vol.68, No.4, p1045-1050.

17. Ito,S.; Adachi, IEEE Trans. Antenna Propagation 1977, Vol.25, No.2, p205-208.

18. Jones,D.S. "The Theory of Electromagnetism", Pergamo: New York, 1964

19. Kanal,M.; Moses,H.E. J. Math. Phys. 1978, Vol.19, No.8, p1793-1798.

20. Kanal,M.; Moses,H.E. J. Math. Phys. 1978, Vol.19, No.12, p2641-2645.

21. Karal,F.C.Jr.; Keller,J.B. J. Math. Phys. 1964, Vol.5, p537-547.

22. Keller,J.B., Proc. Symp. Appl. Math. 1962, 13, p145-170.

23. Keller,J.B., Proc. Symp. Appl. Math. 1964, 16, p145-170.

24. Keller,J.B.; Karal,F.C.Jr. J. Math. Phys. 1966, Vol.7, No.4, p661-670.

25. Kupiec,I.; Felson,L.B.; Rosenbaum,S.; Keller,J.B.; Chaw,P. Radio Sci.1969, Vol.4, p1067-1077.

26. Lang,R.H.; Sokolakis S. Tech. Report ETL-0159, U.S.Army Engineer Topogra. Lab. 1979, Fort Belvoir, VA.

27. Lang,R.H. Radio Science 1981, Vol.16, No.1, p15-30.

28. Lang,R.H.; Sidhu J.S. URSI Commission F Symposium on Signature problem in microwave remote sensing of the surface of earth, 1981

29. Lang,R.H.; Sidhu,J.S. IEEE Trans. Geosci. and Remote Sensing 1983, Vol.GE-21, No.1, p62-71.

30. Lax,M. Review Mod. Phys.1951, Vol.23, NO.4, p287-310.

31. Levine,D.M.; Meneghini,R.; Lang R.H.; Sekar,S.S. NASA TM-83910, 1982

32. Oliver,T.L.; Peake,W.H. Ohio State University, Electro-science Lab., Columbus, OH. Tech. Report 1969 p1903-1909

33. Rosenbaum,S. Radio Sci. 1969, Vol.4, p709-719.

34. Rosenbaum,S.; Bowles,W. IEEE Trans. Antenna Propagation, 1974, Vol.22, No.2, p227-236.

35. Schesser,J.; Eichmann,G. JOSA 1972, Vol.62, No.6, p786--791.

36. Schiffer,R.; Thielheim,K.O. J.Applied Physics 1979, Vol.50, p2476-2483.

37. Shin,R.T.; Kong,J.A. J. Applied Phys. 1981, 52 (6), p4221-4230.

38. Stoggryn,A. Radio Sci. 1974, Vol.9, No.5, p509-518.

39. Tataraski,V.I.; Gertsenshtein,M.E. Sov. Phys. JETP 1963, Vol.17, No.2, p458-463.

40. Taylor,J. "Scattering Theory", John Wiley: New York 1972

41. Tsang,L.; Kong J.A. Radio Sci.1978, Vol.13, No.5, p763-773.

42. Tsang,L.; Kong,J.A. IEEE Trans. Geosci. and Remote Sensing 1981, Vol.19, No.1, p62-69.

43. Tsang,L.; Kubacsi,M.; Kong,J.A. Radio Sci.1981, Vol.16, No.3, p321-329.

44. Twersky,V. J. Math. Phys.1962, Vol.3, No.4, p700-715.

45. Twersky,V. Proc. Symp. Appl. Math. 1964, Vol.16, p84-116

46. Twersky,V. J. Opt. Soc. Am. 1970, Vol.60, No.7, p908-914

47. Twersky,V. J. Math. Phys.1978, Vol.19, No.1, p215-230.

48. Ulaby,F.T.; R.K.Moore,R.K.; Fung,A.K. "Microwave remote sensing, Active and Passive", Vol. 1, Addison-Wesely: MA. 1981

49. Van de Hulst,H.C. "Light scattering by small particles", John Wiley: New York, 1957

50. Zuniga,M.; Habashy,T.; Kong,J.A. IEEE Trans. Geosci. Electron. 1979, Vol.17, No.4, p276-302.

51. Kevorkian,J.; Cole,J. "Perturbation methodsin applied Mathematics", Springer-Verlag, 1981.

52. Smith.D.R. "Singular-perturbation theory - An Introduction with Applications", Cambridge University Press, 1981.